Technical Report Documentation Page

1. Report No. FHWA/TX-00/0-1814-3	2. Government Accession No.	3. Recipient's Catalog No.
4. Title and Subtitle PERFORMANCE OF REHABILITATED LIGHTWEIGHT AGGREGATE ASPHALT CONCRETE PAVEMENTS UNDER WET AND HEATED MODEL MOBILE LOAD SIMULATOR TRAFFICKING: A COMPARATIVE STUDY WITH THE TxMLS		5. Report Date March 2000
7. Author(s) Lubinda F. Walubita, Fred Hugo, and Amy Epps		6. Performing Organization Code
		8. Performing Organization Report No. 0-1814-3
9. Performing Organization Name and Address Center for Transportation Research The University of Texas at Austin 3208 Red River, Suite 200 Austin, TX 78705-2650 Texas Transportation Institute Texas A&M University System College Station, TX 78763 Center for Geotechnical and Highway Materials Research The University of Texas at El Paso El Paso, TX 79968		10. Work Unit No. (TRAIS)
		11. Contract or Grant No. 0-1814
12. Sponsoring Agency Name and Address Texas Department of Transportation Research and Technology Transfer Section/Construction Division P.O. Box 5080 Austin, TX 78763-5080		13. Type of Report and Period Covered Research Report (9/1/98 to 8/31/99)
		14. Sponsoring Agency Code

15. Supplementary Notes
Project conducted in cooperation with the U.S. Department of Transportation, Federal Highway Administration, and the Texas Department of Transportation.

16. Abstract

One-third-scale Model Mobile Load Simulator Mk3 (MMLS3) tests were conducted on US 281 in Jacksboro, Texas, adjacent to the full-scale Texas Mobile Load Simulator (TxMLS). The objectives were to investigate the moisture susceptibility and relative performance of the recently constructed Dustrol and Remixer rehabilitation surface layers and to compare rutting caused by the MMLS3 to rutting caused by the TxMLS. MMLS3 trafficking was conducted under hot (50 °C measured at 25 mm pavement depth) and wet (30 °C measured at 25 mm pavement depth) conditions. The hot tests were run on the surface and a milled pad on both the north- and southbound lanes of the test site. The wet tests were run only on one milled pad in the north- and southbound carriageways. A total of 1.22 million MMLS3 axle loads were applied to the six test pads. Nondestructive stiffness measurements with the portable seismic pavement analyzer (PSPA) and seismic analysis of surface waves (SASW) devices were also performed intermittently during MMLS3 testing. A variety of laboratory tests — volumetrics, moisture sensitivity, shear, indirect tensile strength (ITS) and fatigue, and semicircular bending (SCB) — were also performed.

From the results the relative susceptibility of Dustrol, Remixer, and the in-situ lightweight aggregate asphalt concrete (LWAC) layers to water damage could be determined, with the latter proving the most vulnerable. The MMLS3 and TxMLS deformations in the upper 90 mm surface layers correlated very well in terms of the respective stresses imposed by the two APT devices, after allowing for the difference in environmental conditions during trafficking.

17. Key Words: Accelerated pavement testing, MMLS Mk3, Texas Mobile Load Simulator, wet and heated trafficking	18. Distribution Statement No restrictions. This document is available to the public through the National Technical Information Service, Springfield, Virginia 22161.	
19. Security Classif. (of report) Unclassified	20. Security Classif. (of this page) Unclassified	21. No. of pages 66	22. Price

Form DOT F 1700.7 (8-72)   Reproduction of completed page authorized

PERFORMANCE OF REHABILITATED LIGHTWEIGHT AGGREGATE ASPHALT CONCRETE PAVEMENTS UNDER WET AND HEATED MODEL MOBILE LOAD SIMULATOR TRAFFICKING: A COMPARATIVE STUDY WITH THE TxMLS

by

Lubinda F. Walubita

Fred Hugo

Amy Epps

Research Report Number 0-1814-3

Research Project 0-1814
Project Title: MLS Research Management System — Phase III

Conducted for the

TEXAS DEPARTMENT OF TRANSPORTATION

in cooperation with the

U.S. Department of Transportation
Federal Highway Administration

by the

CENTER FOR TRANSPORTATION RESEARCH
Bureau of Engineering Research
THE UNIVERSITY OF TEXAS AT AUSTIN

and the

TEXAS TRANSPORTATION INSTITUTE
TEXAS A&M UNIVERSITY SYSTEM

and the

THE UNIVERSITY OF TEXAS AT EL PASO

March 2000

DISCLAIMERS

NOT INTENDED FOR CONSTRUCTION, BIDDING, OR PERMIT PURPOSES

Frederick Hugo, P.E. (Texas No. 67246)
Research Supervisor

Research performed in cooperation with the Texas Department of Transportation and the U.S. Department of Transportation, Federal Highway Administration.

ACKNOWLEDGMENTS

TTI -Texas A&M University System: Dr. Dallas Little, Charles (Gene) Schlieker, Sidney Greer, and Paul Nehring
The University of Texas at El Paso: Dr. Soheil Nazarian
CTR-The University of Texas at Austin: Michael E. Gray, Ray Donley, and Pieter Poolman
ITT - Univ. of Stellenbosch: A. D. F. Smit and Prof. M. F. C. Van de Ven
Technical consultants: Bob Sieberg and Johan F. P. Müller

ABSTRACT

One-third-scale Model Mobile Load Simulator Mk3 (MMLS3) tests were conducted on US 281 in Jacksboro, Texas, adjacent to the full-scale Texas Mobile Load Simulator (TxMLS). The prime objectives were to investigate the moisture susceptibility and relative performance of the recently constructed Dustrol and Remixer rehabilitation surface layers and to compare rutting caused by the MMLS3 to rutting caused by the TxMLS. MMLS3 trafficking was conducted under hot (50 °C measured at 25 mm pavement depth) and wet conditions (30 °C measured at 25 mm pavement depth). The hot tests were run on the surface and a milled pad on both the north- and southbound lanes of the test site. The wet tests were run only on one milled pad in the north- and southbound carriageways. A total of 1.22 million MMLS3 axle loads were applied to the six test pads. Nondestructive stiffness measurements with the portable seismic pavement analyzer (PSPA) and seismic analysis of surface waves (SASW) devices were also performed intermittently during MMLS3 testing to monitor changes in the in-situ asphalt concrete (AC) pavement modulus. A variety of laboratory tests — volumetrics, moisture sensitivity, shear, indirect tensile strength (ITS) and fatigue, and semicircular bending (SCB) — were also performed to supplement the field performance results.

On average, the performance of the northbound pavement was found to be poorer than that of the southbound pavement. Analysis of the results indicated that the Dustrol process was more susceptible to moisture damage and less resistant to permanent deformation compared to the Remixer process. By contrast, the Dustrol from the hot, dry trafficked test sections had a better indirect tensile fatigue performance in laboratory testing. Stiffness loss, microcracking, and stripping were evident in the wet MMLS3 tests. In both structures, the in-situ lightweight aggregate asphalt concrete (LWAC) layers exhibited a similar degree of water damage at equivalent MMLS3 axle loads — they were in fact the layers most affected by water. As a result, both structures would have similar fatigue life expectancies if water has the same accessibility into the respective LWAC layers during similar trafficking. It is also apparent that the fatigue life expectancy of AC materials susceptible to moisture damage was significantly reduced by wet trafficking, such that even light axle loads with high tire pressures (690 kPa) caused substantial damage.

The MMLS3 and TxMLS deformations in the upper 90 mm surface layers correlated very well in terms of the respective stresses imposed by the two APT devices, after allowing for the difference in environmental conditions during trafficking. The MMLS3, used in conjunction with nondestructive field and laboratory testing, proved to be a valuable tool for supplementing the TxMLS.

TABLE OF CONTENTS

LIST OF FIGURES

LIST OF TABLES

INTRODUCTION

Stripping was found in the upper layers of the southbound outside lane of US 281, adjacent to the Texas Mobile Load Simulator (TxMLS) test site near Jacksboro, Texas (Smit et al. 1999). This finding led to a preliminary diagnostic study to determine the possible cause. It was found that water ingress into the pavement layers had substantially reduced the indirect tensile fatigue resistance of the lightweight aggregate asphalt concrete (LWAC) located in an underlying layer (Smit et al. 1999). Subsequently, testing with the one-third (1/3) scale Model Mobile Load Simulator Mk3 (MMLS3) was commissioned in 1998 to investigate the stripping phenomenon. This testing was achieved by trafficking the pavement in the field using the MMLS3 with a 1 mm[*] sheet of water flowing across the pavement surface (Smit et al. 1999). The hypothesis was that analyzing the effect of surface water on the performance of the test pads in the northbound lane under MMLS3 trafficking would allow a better understanding of the performance of test pads N1 and S1 under TxMLS trafficking. The other primary objective was to compare the MMLS3 rutting to that of the full-scale TxMLS using dry tests (Hugo et al. 1999, and Smit et al. 1999).

The rutting and spectral analysis of surface waves (SASW) results of the first MMLS3 tests in Jacksboro led to the commissioning of a second set of tests in 1999 (Smit et al. 1999, and Hugo et al. 1999). SASW modulus results, as well as surface microcracking under wet MMLS3 trafficking, had indicated that the asphalt surfacing (overlay) on the northbound carriageway of US 281 was potentially susceptible to moisture damage (Smit et al. 1999). For this reason, additional wet MMLS3 testing was recommended on both the north- and southbound carriageways of US 281 to ascertain whether the overlays were moisture susceptible, given that they had performed relatively well under dry trafficking conditions. This testing was to be achieved by milling off the overlay surfaces and conducting both hot and wet tests on the original and milled surfaces. In the case of the hot dry tests, milling off the top surfaces would also indicate which layer was more susceptible to shear failure and rutting. With the top surfaces milled off, higher MMLS3 stresses would be induced deeper down within the pavement layers. By considering the cumulative effect of tests on the upper and lower layers, it was expected that the comparison of the rutting performance between the two machines would be improved. The 1999 MMLS3 tests in Jacksboro also gave a comparative performance of the two rehabilitation processes, Dustrol and Remixer, used on the northbound and southbound lanes, respectively. The hot tests were conducted to investigate the effects of high temperatures on rutting.

From May 24, 1999, to July 9, 1999, six tests were conducted involving the application of 1.22 million axles. Four hot, dry tests were conducted at 50 $^\circ$C (the temperature being measured at a pavement depth of 25 mm) with a 420 kPa tire inflation

---

[*] Given that researchers working in the area of accelerated pavement testing (APT) use metric units, and given that TRB Task Force A2B52 on APT has set guidelines that include the exclusive use of metrics for capturing APT data, the authors have elected to use metric units exclusively in the report proper.

pressure. Of the four tests, two were carried out directly on the rehabilitated surfaces and the other two were carried out on the surfaces of milled sections of the north- and southbound inner lanes, respectively. The two wet tests (water applied during trafficking) were conducted on the milled surfaces at a temperature of 30 $^{\circ}$C (at 25 mm pavement depth) with a 690 kPa tire inflation pressure. The intent was to do all tests at 690 kPa, but the first hot test was done inadvertently at 420 kPa and accordingly the remainder of the hot tests were done at the same tire pressure to enable comparisons to be made. The axle loading was 2.1kN in all the tests.

Approximately 25 mm of pavement was milled off the northbound section, and about 40 mm was milled off the southbound surface. The test details and number of axles applied on each test pad are summarized in Table 1.

Table 1: MMLS3 test details

Test No.	Test Pad	Surface Type	Test Type	Tire Pressure (kPa)	Target Trafficking Temperature @ 25 mm depth ($^{\circ}$C)	Axles Applied
1	n1	Smooth (Top Surface)	Hot	420	50	320,000
2	n2	Rough (~25 mm milled off)	Hot	420	50	160,000
3	n3	Rough (~25 mm milled off)	Wet (1 mm water)	690	30	320,000
4	s1	Smooth (Top Surface)	Hot	420	50	180,000
5	s2	Rough (~40 mm milled off)	Hot	420	50	80,000
6	s3	Rough (~40 mm milled off)	Wet (1 mm water)	690	30	160,000
					Total axles applied:	1,220,000
Trafficking axle load in kN:						2.1
Temperature tolerance during trafficking:						±2 $^{\circ}$C

This report presents the test objectives, test site location, pavement structures, rehabilitation processes, MMLS3 setup, and methodology and test results of the recent (1999) MMLS3 tests conducted in Jacksboro. Discussions, conclusions, and recommendations follow the description of the testing procedure.

The data collected by the researchers included axle counts; hourly temperature readings; transverse profile measurements using the TxMLS profilometer; longitudinal and transverse Portable Seismic Pavement Analysis (PSPA) and Spectral Analysis of Surface Waves (SASW) measurements at selected grid points; and surface deformation measurements from the small layer deformation pins (LDPs) installed in the pavement prior to testing. The anticipated modes of failure for the hot and wet tests were surface rutting and cracking and stripping, respectively. The results of particular importance for the hot tests

were the surface deformation and pavement temperatures. For the wet tests, the PSPA and SASW moduli measurements, microcrack development, degradation, and stripping were most significant.

Numerous cores were extracted from and within the vicinity of the MMLS3 test pads of both the northbound and southbound pavement structures for material characterization and laboratory testing. Laboratory tests included volumetrics, moisture sensitivity, shear, indirect tensile strength, tensile stresses in SCB mode, and determination of fatigue life in an indirect tensile mode.

TEST OBJECTIVES

The 1999 MMLS3 tests in Jacksboro, in addition to being part of the on-going, full-scale APT program using the TxMLS, represented a continuation of the MMLS3 tests conducted in 1998 under the TxMLS program. The tests were conducted for the Texas Department of Transportation (TxDOT) by the Center for Transportation Research (CTR) of The University of Texas at Austin in collaboration with the Texas Transportation Institute (TTI) of the Texas A&M University System and with The University of Texas at El Paso.

TxDOT launched the TxMLS program in 1995 with the primary objectives of investigating the load damage equivalency, determining remaining pavement life and its impact on rehabilitation guidelines, and investigating new pavement materials and truck component-pavement interaction (Hugo et al. 1999 [b]). The APT test results acquired since then have provided a sound platform for extending new pavement technology, design strategies, and monetary savings.

Using the previous TxMLS results and the 1998 MMLS3 test results (Hugo et al. 1999 [a], [b], and [c]; and Smit et al. 1999), a qualitative comparison of the performance of the rehabilitated LWAC under normalized temperature, pavement structure, and traffic loading had indicated the following:

- The rutting damage power function (n) varied between 4.7 and 6.6.
- Remixer had better rutting performance than Dustrol, but the advantage decreased with axle trafficking. After 1,500k axles, the Remixer had rutted only 3.5 mm, compared with 4.6 mm for the Dustrol.
- The rehabilitation surfaces on both the north- and southbound lanes were susceptible to moisture damage, according to the SASW modulus results.
- The main difference between the performances of the two rehabilitation processes revolved around the upper three layers, which included both the processed rehabilitation layers and the in-situ LWAC.

Based on the above findings, the objectives of the latest (1999) MMLS3 tests in Jacksboro were:

1. To investigate the moisture and rut susceptibility of the overlays, namely, the Dustrol and Remixer processes used on the northbound and southbound lanes of US 281, respectively, and to compare their performances. This finding would further validate the previous findings under the TxMLS testing.
2. To investigate the impact of water on pavement degradation and stripping.
3. To investigate the difference in rutting between the TxMLS and MMLS3. Milling of the upper surface layers would result in higher stress levels under the MMLS3 deeper within the pavement layers, providing for a better comparison with the TxMLS. It would also indicate which layer was most susceptible to shear failure and rutting.
4. To investigate the effects of high temperature and moisture on pavement rutting and microcracking.

The MMLS3 results also provided a comparison with the Hamburg test results that were reported by Hugo et al. (1999). The Hamburg test had indicated that the bottom composite layers (62 mm) were more temperature susceptible than the top 62 mm, and that the northbound pavement structure was more sensitive to temperature than the southbound pavement structure.

Despite limited resources and time, the present test was designed to investigate the performance of the recently rehabilitated upper pavement layers on a limited scale (in terms of numbers of axle loads), taking into account the TxMLS results and the previous MMLS3 test results. Primarily, the idea was to compare the performance trends of the recently rehabilitated upper layers that used the Dustrol and Remixer processes.

TEST SITE LOCATION AND PAVEMENT STRUCTURES

The MMLS3 testing was conducted on highway US 281 near Jacksboro, Texas (the test site was approximately 8 km south of Jacksboro). Highway US 281 is an in-service, four-lane highway with two lanes in either direction (north and south). The Fort Worth district engineer had indicated that there was an average of 3,100 vehicles traveling the highway per day (~1,550 per direction) in 1994, and that approximately 17.4% of the traffic was composed of trucks (Hugo et al. 1998). The north and south lanes are separated by a median approximately 15 m wide and are of different top-material composition, as seen in Figure 1. Accelerated pavement testing was performed on the inner lanes, while the outside slow lanes remained open to traffic.

Prior to the application of the latest rehabilitation processes, the US 281 highway lanes (both north and south) were of similar material composition (Figure 1). Both surfaces consisted of 50 to 75 mm of lightweight asphalt concrete (LWAC, overlaid in 1986), 85 mm of old asphalt surfacings (constructed in 1971 and 1976), and the original 15 mm seal coat, 380 mm flex base, and subgrade (constructed in 1957). The only difference was the depth to the bedrock, which is approximately 2.6 m on the southbound lanes and 1.9 m on the northbound lanes.

In 1971, 1976, and 1986, all the US 281 lanes were given a similar rehabilitation treatment of ordinary asphalt concrete (AC), composite aggregate AC, limestone AC, and lightweight aggregate asphalt concrete pavement (ACP), respectively. In the latest rehabilitation operation, the northbound and southbound lanes were overlaid differently using the Dustrol and Remixer processes, respectively.
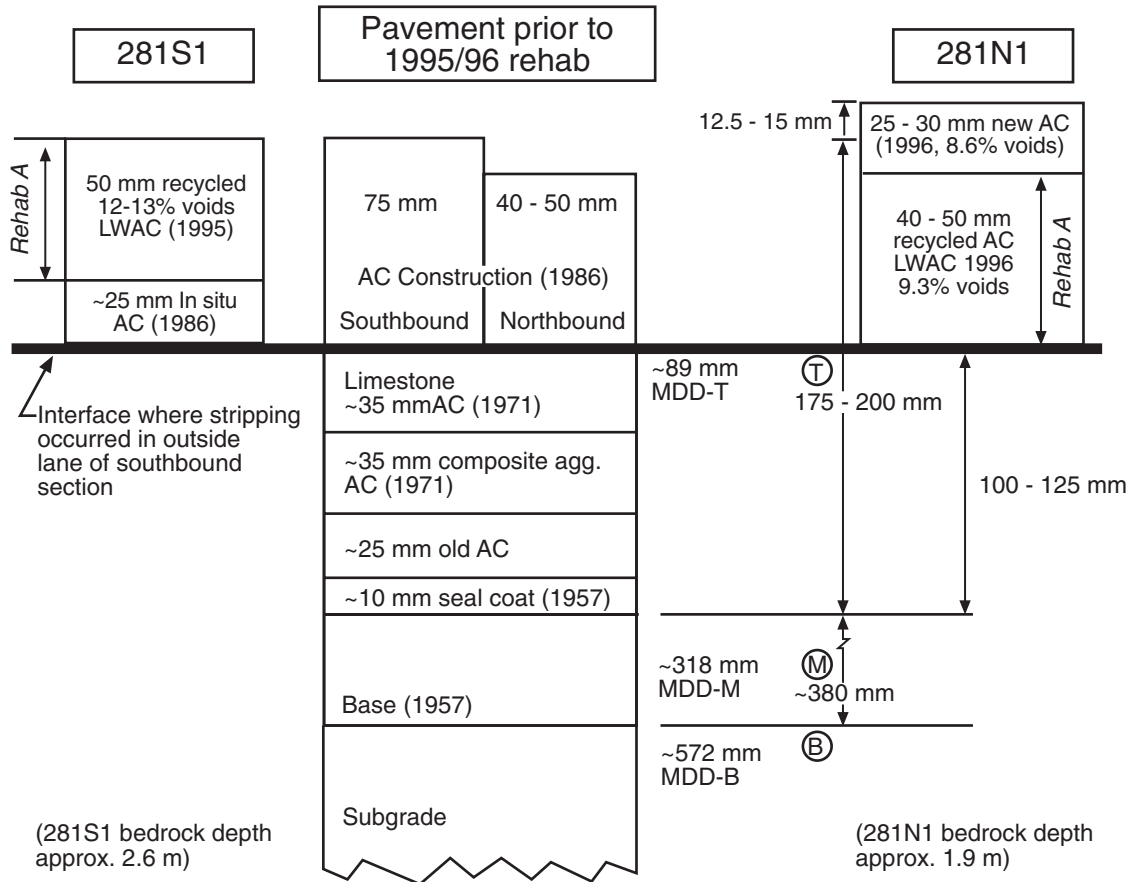
Figure 1: US 281 pavement structures

THE REHABILITATION PROCESSES

The two rehabilitation processes are discussed below.

US 281 Northbound Lanes (Dustrol)

The northbound lanes were reconstructed in 1996 using a Dustrol process. This reconstruction entailed scarifying the LWAC in situ and treating it with Reclamite (a rejuvenating oil) before compaction. Thereafter, it was overlaid with conventional limestone

AC (about 25 mm thick). The conventional ACP had an air void content of approximately 8.6%. Below the 25 mm thick conventional ACP is approximately 45 mm of LWAC, of which the upper 25 mm was processed.

During the diagnostic studies the researchers found that there was a difference in the layer structure between the left and right wheelpaths of the trafficked inner lane. The right wheelpath cores had a distinct 25 mm top limestone AC surfacing layer, while the left wheelpath cores had an average 15 mm thickness, particularly in the case of the 1998 dry MMLS3 test section (Smit et al. 1999). This finding is discussed in more detail in the materials and laboratory testing section of this report.

US 281 Southbound Lanes (Remixer)

The two southbound lanes were rehabilitated in 1995 using the Remixer process, which is a 50 mm (nominal) overlay of recycled and repaved lightweight aggregate with some fresh limestone AC added along with a dosage of Reclamite. The average air void content was about 12.5%. Immediately below the Remixer is an approximately 20 mm thick in-situ LW AC layer.

MMLS3 TEST SETUP AND METHODOLOGY

The one-third (1/3) scale MMLS3 is a low-cost APT device that applies a maximum of 7,200 single-wheel applications per hour. It is a unidirectional, scaled-down vehicle-load simulator used for accelerated trafficking of model or full-scale dry and wet pavements. The MMLS Mk3 machine is shown in Figure 2, and its technical features are tabulated in Table 2. Further MMLS3 details have been published elsewhere (Smit et al. 1999). The MMLS3 loading speed is about 2.5 m/s (9 km/hr), which is equivalent to a frequency of approximately 4 Hz (Smit et al. 1999).

Once on site, the researchers' first step was to select a suitable test section and mark it. The MMLS3 test pad was a rectangular section 500 mm wide by 1,200 mm long, with transverse gridlines at 200 mm intervals, as shown in Figure 3. The grids were marked by painting for easy positioning and centering of the MMLS3 machine, installation of the small LDPs and thermocouples, and taking of profilometer, PSPA, and SASW measurements.

It is recommended that test personnel always select a flat area with even surface (and uniform material properties) as the MMLS3 test site so as to ensure a uniform surface-contact load and comprehensive results. Such a site also facilitates easy MMLS3 setup and trafficking. A flat, even surface also reduces mechanical problems during trafficking and facilitates easier measurements. Dynamic load effects are also minimized. In addition to these requirements, the surface also had to be crack-free with no visible ruts. The presence of non-MMLS3 associated cracks and ruts could adversely affect the final results (i.e., the defects could exaggerate the MMLS3 trafficking effect on the pavement and thus distort the results).

It is also important that researchers perform radar scanning and coring for material characterization tests to determine the homogeneity of the pavement materials and to provide insight about the expected performance prior to selecting the pads. This exercise is particularly important if the test-pad performances are to be compared. Prior knowledge of the pavement layer structure, such as thickness details, is also necessary.

(a) Side-1   *(b) Side-2*
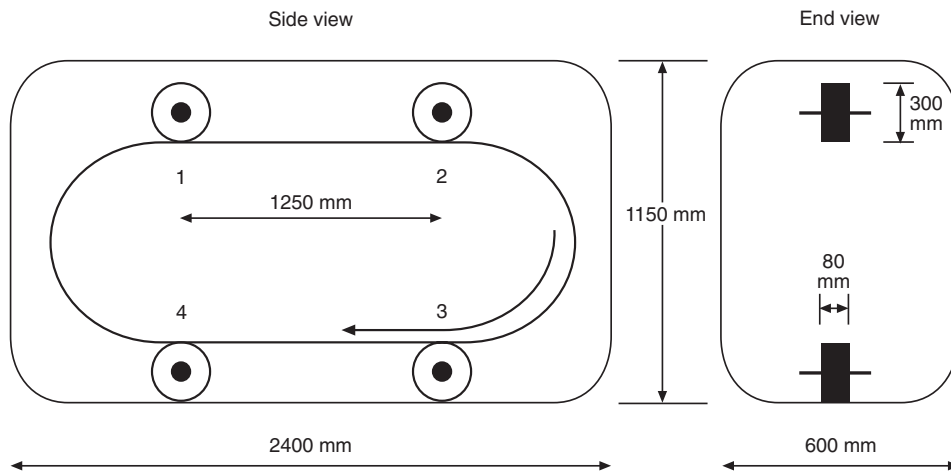
(c) Schematic view of the MMLS3

Figure 2: The MMLS3

Table 2: MMLS3 load configuration and technical data

FEATURE	TECHNICAL DATA
No. of bogies	4
No. of axles per bogie	1
Total number of tires	4
No. of tire per axle	1
Tire type	4.00-4, pneumatic rubber, 300 mm diameter

FEATURE	TECHNICAL DATA
Maximum tire pressure (kPa)	800
Nominal tire width (mm)	80
Nominal wheel diameter (mm)	300
Tire foot print area (mm^2)	3400
Nominal maximum load per axle (kN)	2.7
Nominal maximum load per wheel (kN)	2.7
Maximum wheel loads per hour	7200
Load mechanism	Spring controlled
Load setting	Suspension-spring system
Suspension	Steel springs
Load control	Automatic (constant load)
Nominal Speed (unidirectional travel of wheels)	2.5m/s (about 4 Hz equivalent)
Duration of load pulse at operational speed (sec)	0.016
Nominal rest periods between load applications (sec)	0.5
Nominal time per cycle (sec)	2
Control Unit Housing — dimensions (mm)	400 x 500 x 200
— color	Electric orange
— special features	IP65 weather proof metal box
Supply Voltage	220 volts, 50/60 Hz AC (single phase)
Power Consumption	1500 watt maximum, 1.5 (7 amp)
Lateral wander on each side of centerline (mm)	80 (right and left)
Total maximum track width (mm)	240
Mobility	towed whilst supported on wooden base
Movement	On own wheels or by crane
Overall operational machine dimensions (mm):	2400 mm long x 600 mm wide x 1150 mm high
Total operational dead weight (kg)	672
Total nominal mass (kg)	800
Test section size (mm)	1200 x 500
Temperature control during tests	3100 mm long x 1250 mm wide x 1310 mm high x 90 mm thick temperature chamber with an automatic controlled heating unit
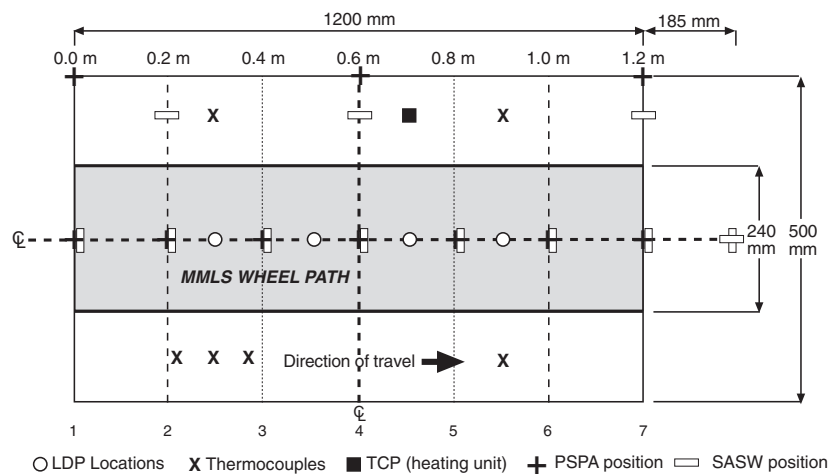
Figure 3: MMLS3 test grid

Once a test pad had been selected and marked by painting, four small LDPs were installed on the center-longitudinal grid line to measure the relative deformation of the pavement layers with MMLS3 trafficking. Thermocouples were then installed at various depths within the pavement structure to monitor the pavement temperature. Two temperature probes were used for measuring the temperature. The thermocouple and LDP positions are shown in Figure 3, and their details are shown in Figures 4 and 5, respectively.
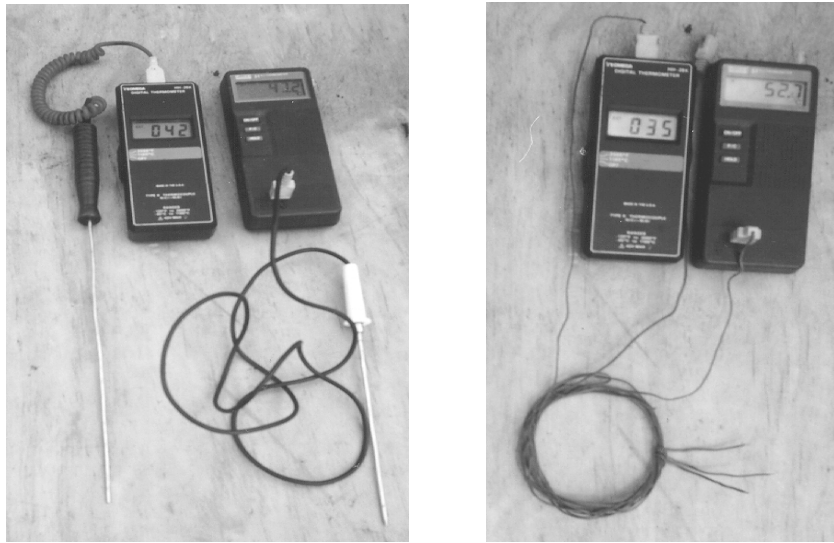
Figure 4: Temperature probes and thermocouple wires
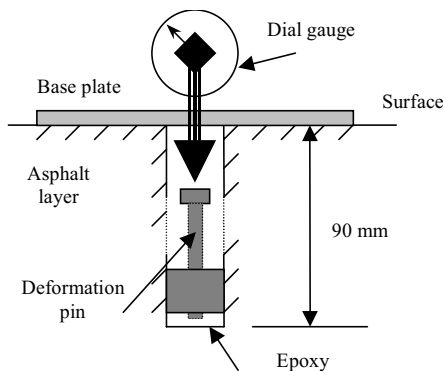
Figure 5: LDP gauge and installation details

Finally, the profilometer guide rails used in taking profile measurements were fixed into the pavement (with nails) longitudinally along the test pad. The test pad was then thoroughly swept in preparation for taking the initial zero (0k) measurements. An air compressor was also used for blowing away loose particles from the test pads prior to MMLS3 trafficking and measurements. (Loose particles on the test pad surface distort profilometer readings.)

The research team positioned the MMLS3 machine on the test pad by longitudinally and transversely centering it along the two centerlines (longitudinal and transverse) of the test pad. Next, the researchers detached the machine's mobility wheels and set the machine on the test pad as described in the MMLS3 operations manual (Muller 1999 and Smit et al. 1999).

Hot Tests

For the hot tests (n1, n2, s1, and s2), the MMLS3 machine and test pad were covered in the temperature chamber prior to commencement of trafficking and were heated until the desired 50 ± 2 $^{\circ}$C trafficking temperature at 25 mm depth was reached. The average heating time prior to the start of trafficking was 5 hours. To maintain the 50 $^{\circ}$C trafficking temperature, heating continued throughout the MMLS3 runs. The heating unit had an automatic control thermostat to regulate the heating process. It was set to a control temperature of 55 $^{\circ}$C with a differential temperature range of 2 $^{\circ}$C. The thermostat probe (TCP) was embedded at a depth of 10 mm within the test pad. The pavement was heated so researchers could traffic the surface at a temperature more realistically related to the critical temperature of the asphalt mix for the region. The heating unit and the temperature chamber are shown in Figure 6.

(a) Heating unit   *(b) Temperature chamber*

Figure 6: The MMLS3 heating system

Wet Tests

MMLS3 trafficking commenced almost immediately after setup for the wet tests (n3 and s3). Heating was in most instances unnecessary, as the temperature at the 25 mm depth was normally at the desired trafficking temperature of 30 ± 2 $^{\circ}$C. During trafficking, an approximately 1mm thick sheet of hot water (about 45 $^{\circ}$C) flowed across the milled test pads. The application of hot water also aided in maintaining the 30 $^{\circ}$C trafficking temperature.

Milled Test Pads

On the northbound sections, the top 25 mm overlay of limestone AC was milled off to allow trafficking to be conducted on the surface of the LWAC (the second Dustrol layer) on test pads n2 (hot) and n3 (wet). In the southbound structure, s2 (hot) and s3 (wet) had a nominal 40 mm top surfacing of Remixer layer milled off. The intention was to traffic the second LWAC underlying layers and to compare their response to that of the new rehabilitation surfaces. Prior to the marking and painting of these four test pads, an effort was made to smooth the rough milled surfaces using an electric grinder. This was necessary to have a uniform contact load with the surface and reduce the possibility of dynamic load variations.

MMLS3 TEST OPERATIONS

During MMLS3 trafficking, the machine was stopped hourly to check the tire pressure, tires, and rims. Rim bolts and nuts frequently sheared off during trafficking on the rough milled surfaces (n2, n3, s2, and s3), resulting in skew of the rims and tire punctures. This problem necessitated the hourly check of the MMLS3.

For operations on the s-test pads (southbound lane), traffic cones had to be put on the road at around 6 a.m. or 7 a.m. and removed at 5 p.m. or 6 p.m. for traffic control. Sand and 25 mm thick steel plates (Figure 7) were used for covering the milled test pads (s2 and s3) to allow traffic flow after working hours, at night, and during weekends and holidays. The sand was intended to prevent the steel plates from resting directly on the pads. It also cushioned the test pads against any form of non-MMLS3 induced distress or damage that could result from uneven contact with the steel plates. After work hours and during weekends, the MMLS3 machine was moved to the northbound lane and onto the n-test pads for continued trafficking. The inner northbound lane was permanently closed to traffic at the test site.

FIELD MEASUREMENTS AND DATA COLLECTION

The data collected included axle counts, hourly temperature measurements, surface ruts, pavement in situ stiffness, pavement layer deformation, and visual monitoring of cracks and stripping. In this report 'k' stands for one thousand (x 1000).

Southbound lane

Figure 7: Steel plates on Test Pads s2 and s3 (the holes and grooves were used for chain lifting the plates using the TxDOT crane)

In addition to air temperature, measurements were taken for the temperature at the pavement surface (TS), temperatures at depths of 25, 75, and 95 mm from thermocouples (T1, T2, and T3), and the temperature at a 10 mm depth from the heating unit control pin (TCP) (Table 3).

Seven transverse surface profile measurements were taken along the test grids using the TxMLS profilometer (Figure 8). The profilometer computer data-acquisition system captured data at intervals of 10 mm. The profilometer measures to a positional accuracy of ±0.2 mm. It measures changes in height relative to a position that is assigned fixed coordinates (the lower right point on the test grid).

Figure 8: The profilometer

Table 3: MMLS3 trafficking temperatures and ruts at termination of tests

No:	Test Pad	Axles	Mean MMLS3 Trafficking Temperatures (°C)						Maximum Rut (mm)
			Air	TS (0mm)	T1 (25mm)	T2 (75mm)	T3 (95mm)	TCP (10mm)	
1	N1	320,000	29.9	56	49.23	40.29	38.6	49.9	2.2
2	N2	160,000	29.8	57	49.8	42.4	40.1	53.4	2.7
3	N3	320,000	29.0	33	30.3	30.9	29.5	00.0	2.4
4	S1	180,000	38.5	57	50.3	43.5	41.2	53.2	0.6
5	S2	80,000	43.7	57.8	50.3	43.6	41.4	53.7	1.3
6	S3	160,000	40.0	32	30.2	30.6	29.1	00.0	1.1
Overall Mean MMLS3 Trafficking Temperatures	Hot Tests	35.5	56.9	49.9	42.4	40.3	52.5		
	Wet Tests	34.5	32.5	30.25	30.7	29.30	00.00		

PSPA measurements (Figure 9) were taken at seven longitudinal and seven transverse positions along the test grid on the centerline to monitor the change in in situ pavement AC modulus with MMLS3 trafficking. Grid positions 250 mm to the left of the trafficking line (centerline) were used as control points. Three longitudinal and three transverse PSPA measurements were taken from the control grid line at 0 m, 0.6 m, and 1.2 m, respectively. Thus, for each set of PSPA measurements, twenty readings were taken — ten longitudinal and ten transverse. Air and pavement surface temperature measurements were also taken during PSPA measurements, precisely before and after the PSPA measurements. Accordingly, there were four temperature readings for each set of twenty PSPA readings: two for air and two for the pavement surface.

Sets of SASW measurements and corresponding pavement surface temperatures were taken for each test pad at selected points. Like the PSPA, the SASW measures stiffness relative to wave velocity through the pavement. The SASW device is shown in Figure 9 with a dispersion curve in the computer window.

The relative deformation of the pavement layers was measured with the LDPs and the small layer deformation gauge (Figure 5) whenever profilometer readings were taken. The LDPs were installed at the following depths within the test pads: 25, 50, 70, 85, and 90 mm. The depths were selected to obtain information at layer interfaces, and to enable a well-distributed profile of deflection with depth to be established.

(a) PSPA *(b) SASW*

(c) Taking PSPA measurements (on n1) *(d) SASW wave display*
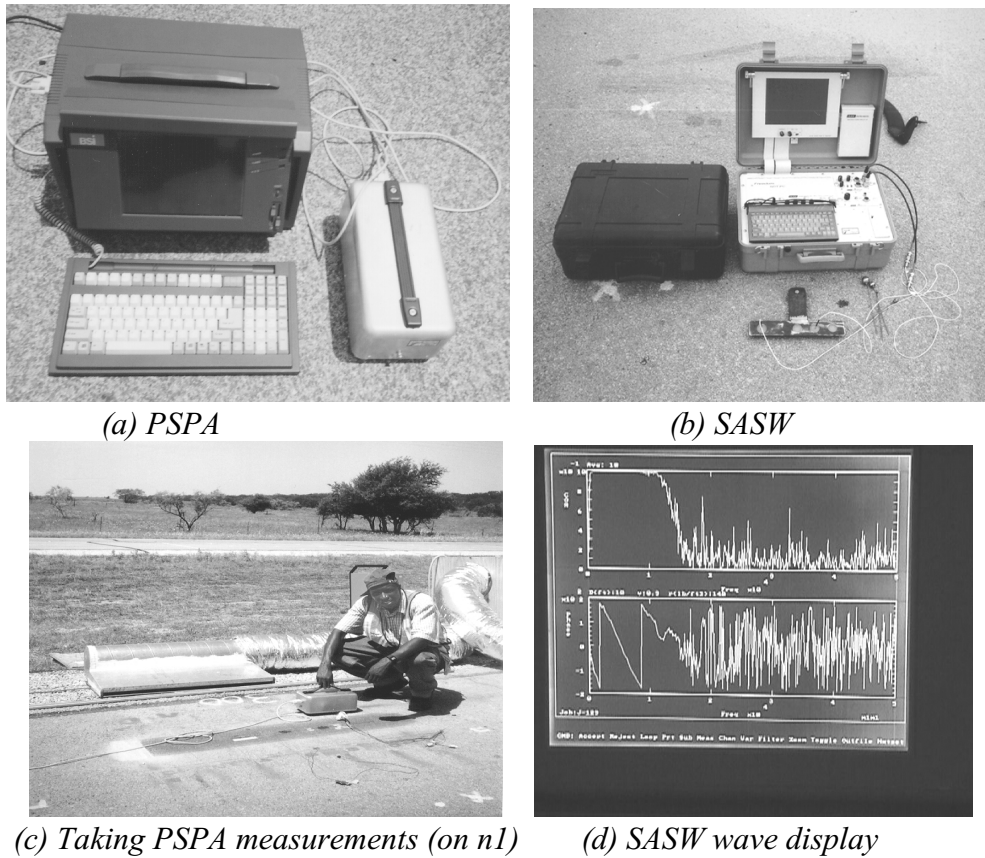
Figure 9: The PSPA and SASW devices

MMLS3 TIME PRODUCTIVITY

After a specific number of axles had been applied, the MMLS3 machine and the heating unit (in the case of the hot tests) were stopped and the whole setup (MMLS3 machine, heating unit, and temperature chamber) was removed from the test pad. Data were collected and then the machine (together with its heating accessories, for the hot tests) was replaced onto the test pad for continued trafficking. This procedure was repeated for each test pad until a target axle count was reached or the testing was terminated. The target axle count was considered such as would yield meaningful rutting in accordance with theoretical predictions.

The n-tests on the northbound lane ran from the end of May to mid-June 1999, with a total application of 800,000 axles. A total of 420,000 axle loads was applied on the s-tests (southbound lane) from mid-June to July 9, 1999.

During trafficking, the MMLS3 was interrupted only for hourly inspections, measurements at the end of target axle counts, and mechanical breakdowns. Mechanical

problems encountered on the milled test pads were due to the uneven surface. Figure 10 shows the breakdown of the entire test period into test setup, heating, MMLS3 trafficking, data collection, maintenance, and nonoperational time.
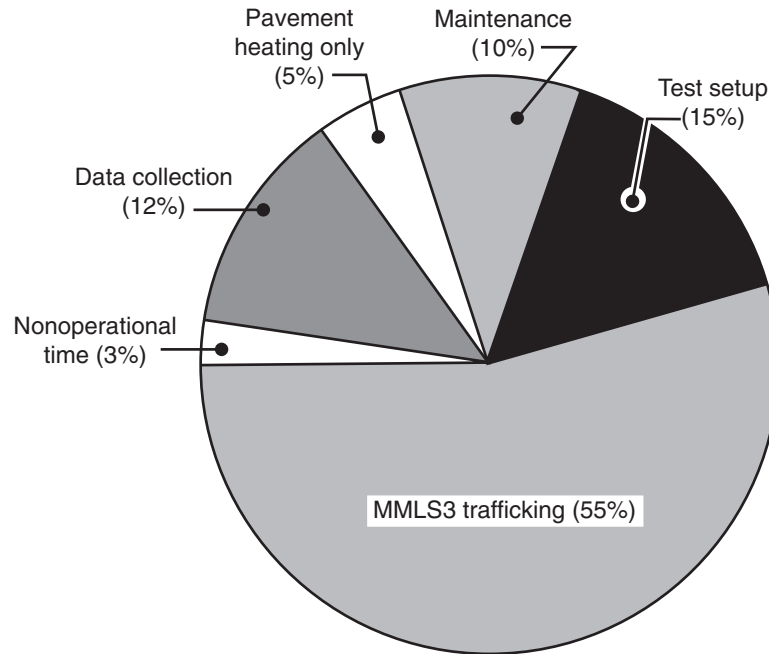
Figure 10: MMLS3 time productivity pie chart

Test set-up time included test site selection, test pad marking, grinding, LDP and thermocouple installation, power supply setup, MMLS3 and heating system setup, removal and replacement of traffic cones and sand and steel plates on the road and milled test pads, respectively, and obtaining hot water.

Maintenance included MMLS3 inspection and repair to the machine. A substantial amount of time was spent on maintenance, particularly on the milled test pads. The major mechanical problems experienced were snapping of the internal drive belt, shearing off of rim bolts and nuts, skewing and ripping off of rims, and puncturing of tire tubes. These problems were subsequently addressed with the switch to more robust wheel rims.

One minor electrical problem experienced was fusing, a problem that was probably due to overload caused by the drive wheels' failure to rotate, which resulted in more electrical power being drawn from the power source. No water-related problems were encountered.

Nonoperational time is defined as that time during the test period when the machine was intentionally not run. This time includes the time when there was no power supply and time during thunderstorms and rainfall.

As can be seen from the time pie chart (Figure 10), the test set-up (15%), data collection (12%), and maintenance (10%) times were relatively high. The high set-up time arose from the MMLS3 setup on the milled southbound test pads, including traffic control and handling of the sand and steel plates. Measurements on the milled surfaces likewise required extra care and precision. PSPA measurements had to be repeated several times to get good readings. The high maintenance time was basically due to the mechanical problems mentioned.

Overall, 60% of the total test period time was spent in active heating and MMLS3 trafficking, and 40% was spent on test setup (15%), data collection (12%), maintenance (10%), and nonoperational time (3%).

LABORATORY TESTING AND MATERIAL CHARACTERIZATION

Several laboratory tests were conducted to supplement the MMLS Mk3 field tests and to characterize the pavement materials. This provided information concerning

- volumetric properties of the materials;
- the shear and elastic stiffness, as well as the phase angle, of AC at different temperatures and loading frequencies;
- material strength before and after MMLS3 trafficking under different conditions (hot, dry, and wet);
- the remaining fatigue life after MMLS3 trafficking, as well as relative fatigue damage caused by MMLS3 trafficking; and
- susceptibility to water damage.

The laboratory results served as an assessment of the material resistance to permanent deformation, loss in strength, degradation, stripping, and MMLS3 traffic damage under different conditions (hot, dry, and wet). This greatly enhanced insight into the field performance of the three upper layers of asphalt concrete under MMLS3 trafficking.

Coring

Cores 100 mm and 150 mm in diameter, with an average length of 100 mm, were taken from within the eight test pads (n1, n2, n3, s1, s2, s3, n-dry, and n-wet) and from outside the test pads from untrafficked sections. At least four cores were extracted from each test pad and four from the untrafficked sections of each of the two lanes (northbound and southbound). Test pads n-dry and n-wet refer to MMLS3 tests that were performed in 1998 by Smit et al. (1999).

Specimen Preparation

During specimen preparation, cores were cut to the required thickness as per pavement-structure layer thickness, and those needing conditioning (i.e., temperature and wetting) were conditioned for a specified number of hours prior to the execution of the actual test. Only the three uppermost layers, up to a total depth of 70 mm, were tested. The core-layer designations and average thicknesses are shown in Figure 11. The core specimens from the top surface layers were denoted 'S' or 'L1' for surface or layer 1, respectively. Specimens from layers 2 and 3 were labeled 'L2' and 'L3,' accordingly. 'C' was used to denote specimens of composite material, such as a combination of layers 1 and 2. 'L*' designates a composite layer comprising L2 and L3. The actual average specimen thickness was 20 mm, except where otherwise designated.
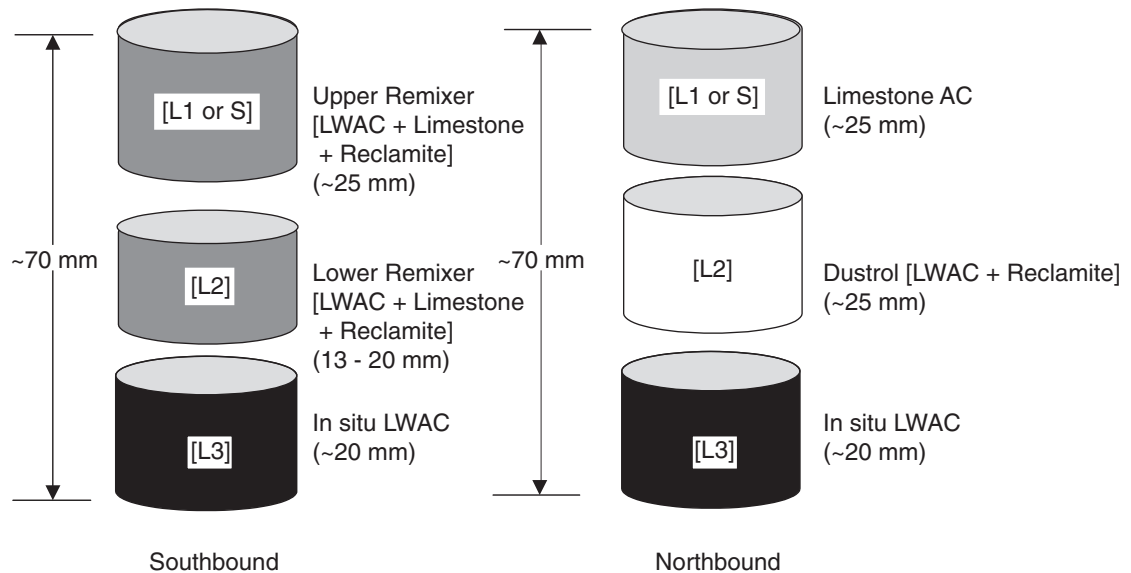
Figure 11: Core-pavement structures

Cores were labeled using the following notations: small "s" for southbound; small "n" for northbound; "u" for untrafficked; "d" and "w" for dry and wet pads, respectively (Smit et al. 1999). So "su" and "nu" define untrafficked cores from the southbound and northbound structures, respectively, and "nd" specifies a core from the dry test from the northbound structure. "su2-L1" defines untrafficked southbound core number 2 from layer 1 (or the surface layer if "S" is denoted). These "core" denotations should not be mixed with the 1999 "test pad" labels (n1, s1; n2, s2; and n3, s3), which denote surface hot; milled hot; and milled

wet tests for the north- and southbound sections, respectively. In both the core and test pad labeling, "n" and "s" define north- and southbound, respectively.

For the northbound structure (trafficked inner lane), the top surfacing-layer thickness from the right wheelpath cores was 25 mm or more. For the left wheelpath cores, it varied and was not well defined on some sections. For cores from the 1998 dry section, the average thickness was 15 mm, and the top surfacing layer was highly inter-mixed with the underlying LWAC. This difference in layer structure probably influenced both the MMLS3 trafficking and laboratory test results.

Laboratory testing was performed by TTI (Texas) and the Institute for Transport Technology (ITT), South Africa.

RESULTS AND DATA ANALYSIS

1. Temperature Profiles

The mean MMLS3 trafficking temperatures for the hot and wet tests, including the air temperature, are presented in Table 3. Figure 12 shows the temperature profile within the pavement layers up to a depth of about 180 mm, at the base of the AC material. Beyond the 180 mm depth is the seal coat, flex base, subgrade, and bedrock. The properties of these layers are for the most part insensitive to temperature.
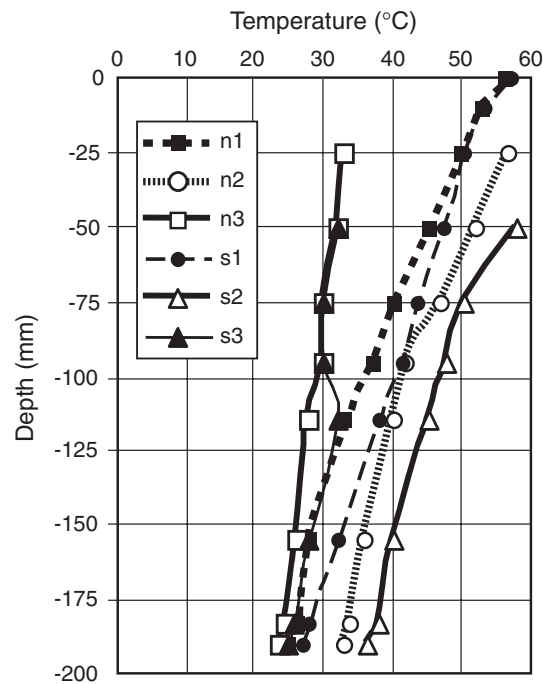
Figure 12: Temperature profiles

18

Hot Tests (Pads n1, n2, s1 and s2)

Three thermocouples embedded at depths of 25, 75, and 95 mm were used for monitoring the temperature variation within the pavement layers on an hourly basis. The overall mean MMLS3 trafficking temperatures were 49.9 °C at the 25 mm depth, 42.5 °C at the 75 mm depth, and 40.3 °C at 95 mm. The temperatures remained fairly constant with minimal variation during trafficking. The temperature gradient decreased with depth, with the highest variation at the 25 mm depth (±1.5 °C) and the lowest at the 95 mm depth (±0.5 °C). The mean control temperature for the heating unit thermostat was 52.6 °C, but the temperature occasionally rose to as high as 57 °C. Figure 13 shows the MMLS3 trafficking temperatures for the hot tests. The mean pavement surface temperature within the temperature chamber during trafficking was 56.9 °C, while the maximum recorded temperature was 60 °C on s1.
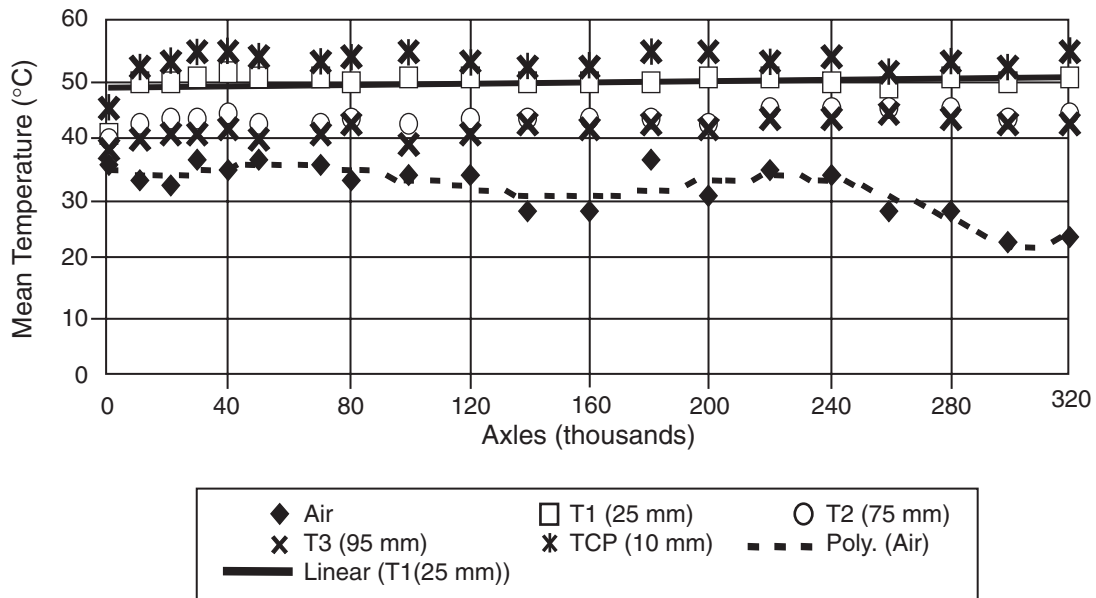
Figure 13: Mean MMLS3 trafficking temperatures for the hot tests

The mean air temperature during MMLS3 trafficking was 35.5 °C. The air temperature was generally low at the start of the tests in May and June, particularly for the n-tests, but it increased to as high as 47 °C in July toward the onset of the summer season. The s-tests were subsequently run at air temperatures higher than those for the n-tests. Such temperatures affected only the amount of heating required during testing.

The daily air temperature variation was cyclic, with the highest temperatures reached at noon (midday) and the lowest at midnight. The highest temperature recorded was 47.6 °C, and the lowest was 18.2 °C. Figure 14 shows a typical example of the daily air temperature

variation during MMLS3 trafficking. A fifth-order polynomial trend line is added to emphasize the cyclic daily air temperature variation.
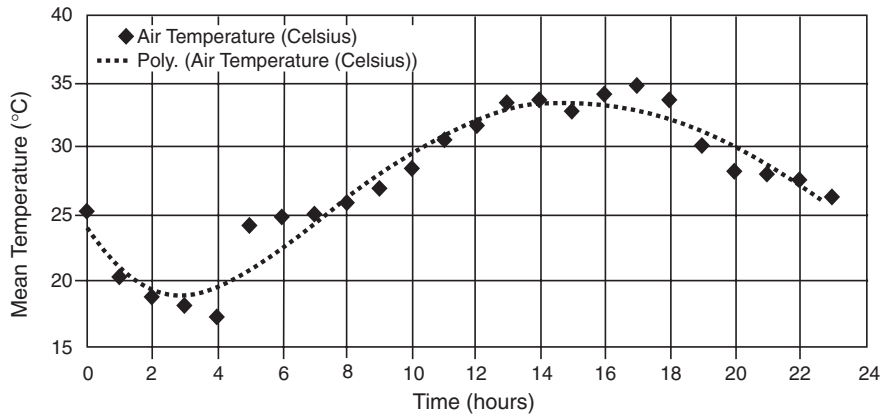
Figure 14: Example of the daily air temperature variation during MMLS3 trafficking

As shown in Figure 14, the lowest temperature recorded was at 3:00 a.m. and the highest around 2:00 p.m. It should be noted that trafficking was also performed at night on the northbound lane, which was permanently closed to conventional traffic at the test section.

Wet Tests (Pads n3 and s3)

Figure 15 shows temperature profiles for the wet tests. The thermocouple setup was similar to that of the hot tests, and the 25 mm depth target MMLS3-trafficking temperature was 30 ± 2 $^{\circ}$C. This temperature was maintained through the use of hot water (about 1 mm thick at 45 $^{\circ}$C) and occasional heating aided by the natural hot weather as the summer season approached.

The daily air temperature variation followed a cyclic trend just as the hot tests did, with the highest recorded air temperature being 46.1 $^{\circ}$C and the lowest 17.2 $^{\circ}$C.
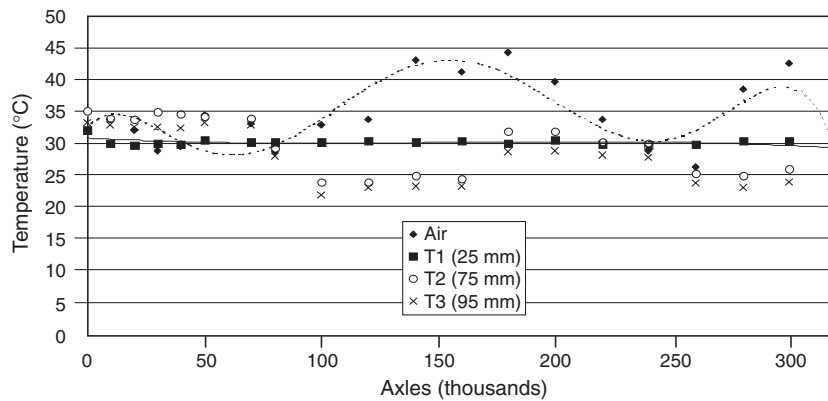
Figure 15: Mean MMLS3 trafficking temperatures for the wet test

2. Surface Rutting

Figures 16 to 20 show the maximum surface rut profiles for the test pads. The ruts presented in this report are the mean maximum determined at the 0.4 m, 0.6 m, and 0.8 m transverse grid lines. On the milled pads, the transverse grid lines 0.2 m, 0.4 m, 0.6 m, 0.8 m, and 1.0 m were used to determine the mean maximum ruts to counter the unevenness of the top surface.
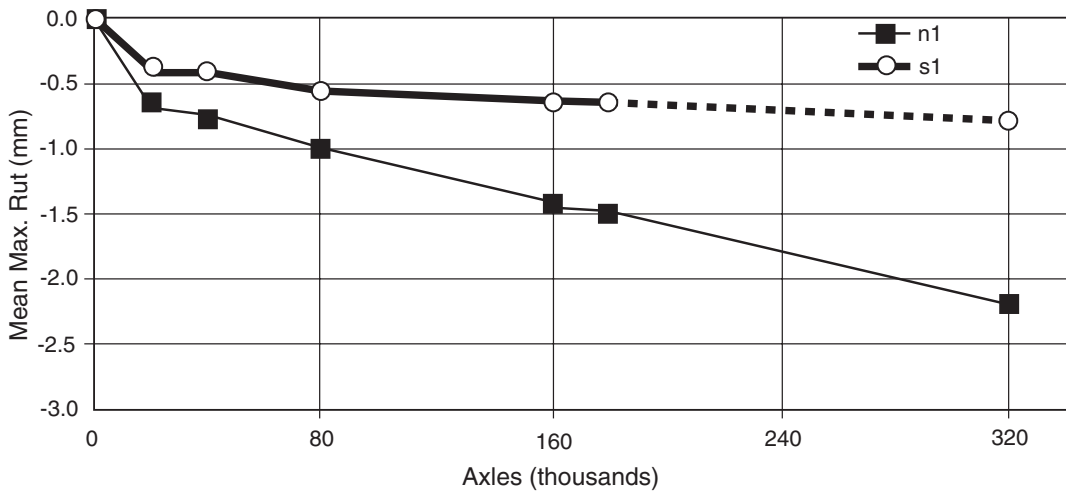
Figure 16: n1 and s1 ruts
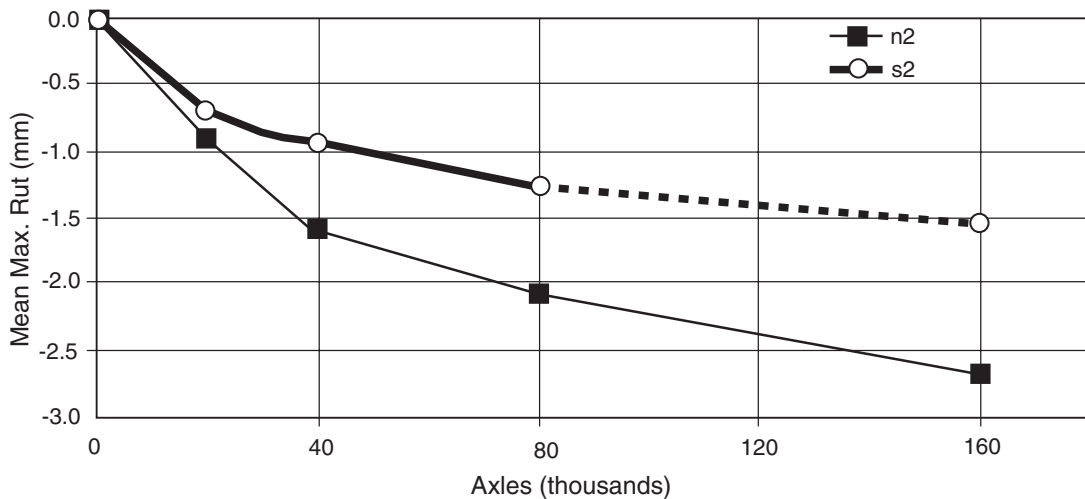
Figure 17: n2 and s2 ruts
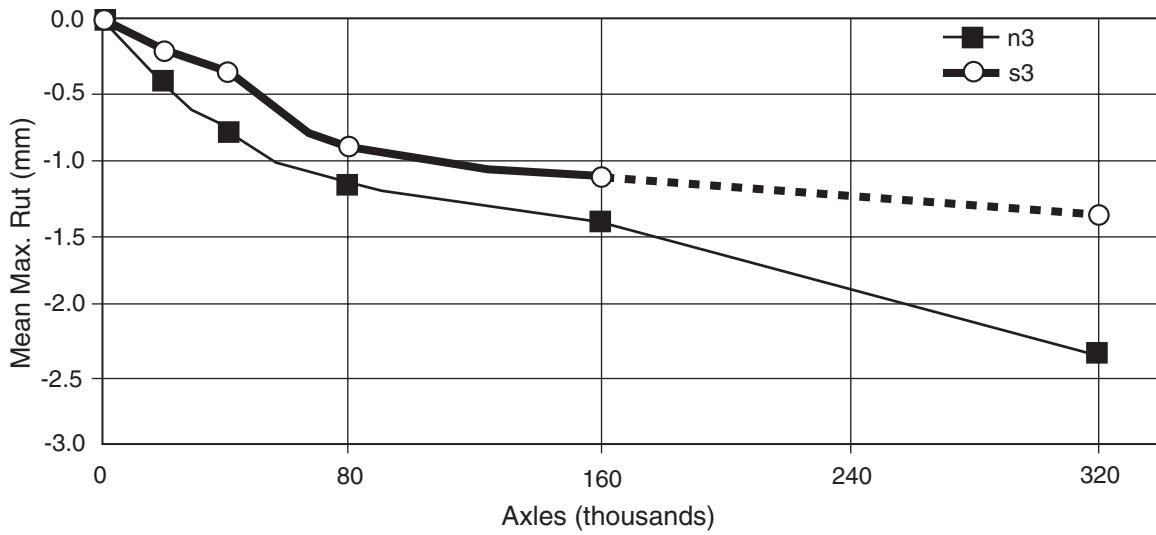
Figure 18: n3 and s3 ruts
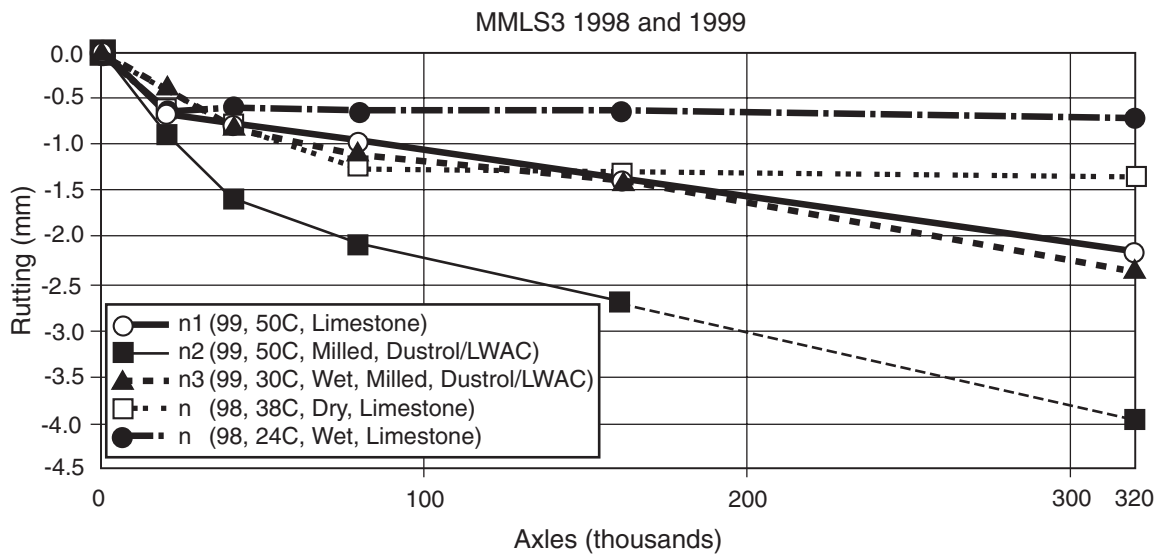
Figure 19: MMLS3-1998 and MMLS3-1999 ruts

22
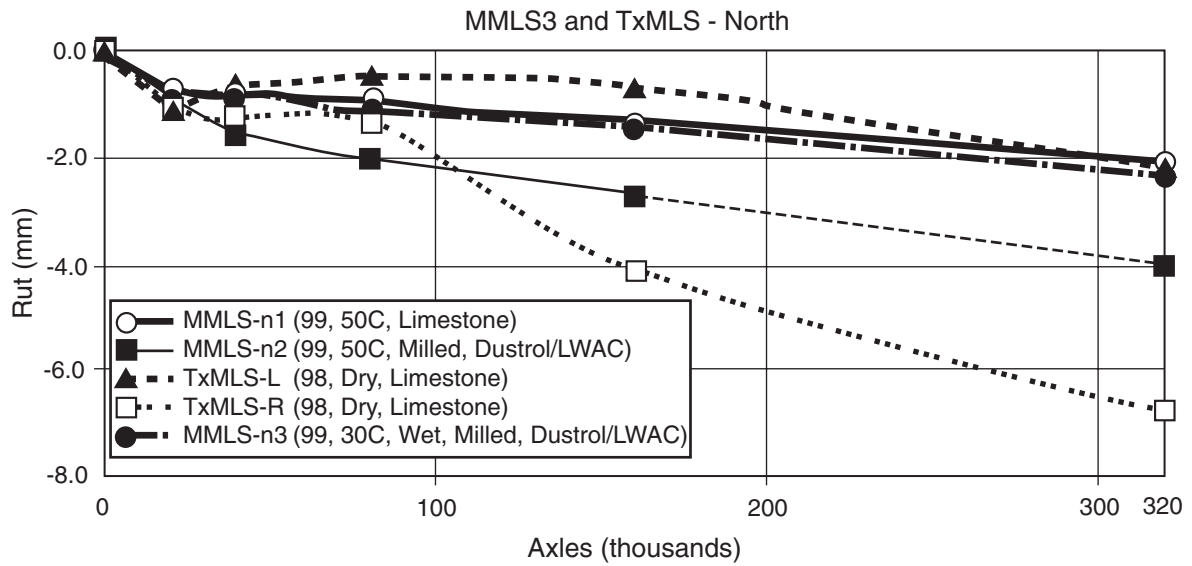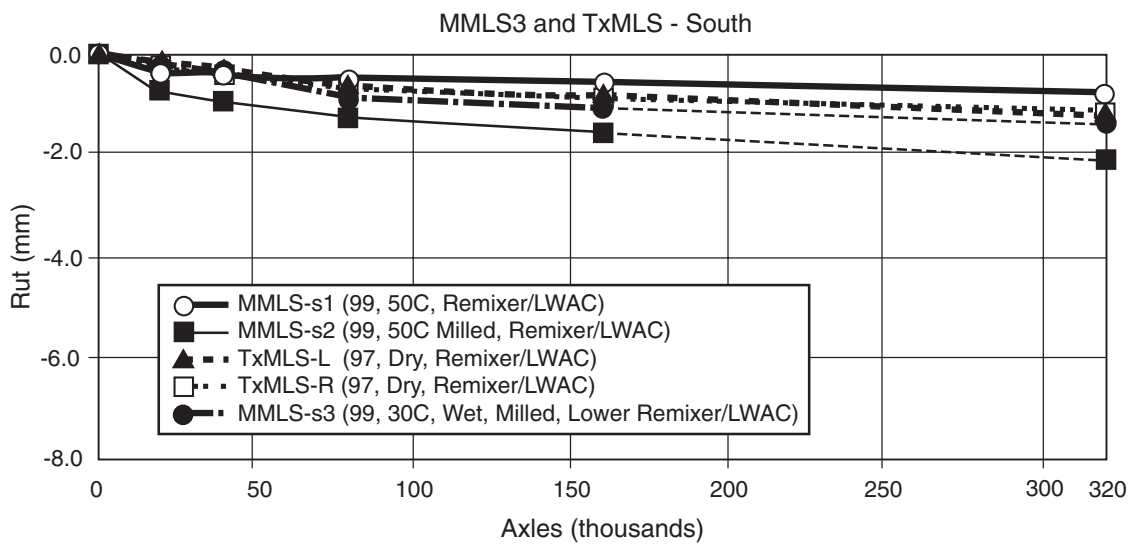
(a): Northbound lane

(b): Southbound lane

Figure 20: TxMLS and MMLS3 ruts

The Northbound Lane (Pads n1, n2 and n3)

After 160k, the ruts in n1, n2, and n3 were 1.39, 2.69, and 1.40 mm, respectively. At 320k, the rut depth on n1 was 2.17 mm and the rut depth on n3 was 2.35 mm. It was clearly evident that the in-situ processed Dustrol and LWAC layers (n2 and n3) were less resistant to permanent deformation than the limestone AC overlay. The layers were highly sensitive to temperature and susceptible to water damage.

Dynamic effects related to the rough surface could have caused some of the increased rutting in milled pads n2 and n3 (compared to n1). However, this is not likely, because the MMLS3 wheel load was found to vary by no more than 5%, with a difference in vertical height movement of about 20 mm. Nevertheless, in future test preparation of milled surfaces, greater care should be taken to counter any possible effects of the uneven surface.

Figure 21 shows the milled pads n2 and n3. The change in tire pressure to 690 kPa could have contributed to the greater rutting in n3 than that in n1. At the same temperature, this would have increased the rutting by more than 60%. However, the lower temperature of pad n3 would have mitigated this effect. Therefore, no correction was made.

(a) n2, 2.7 mm @ 160k   *(b) n3, 2.4 mm @ 320k*
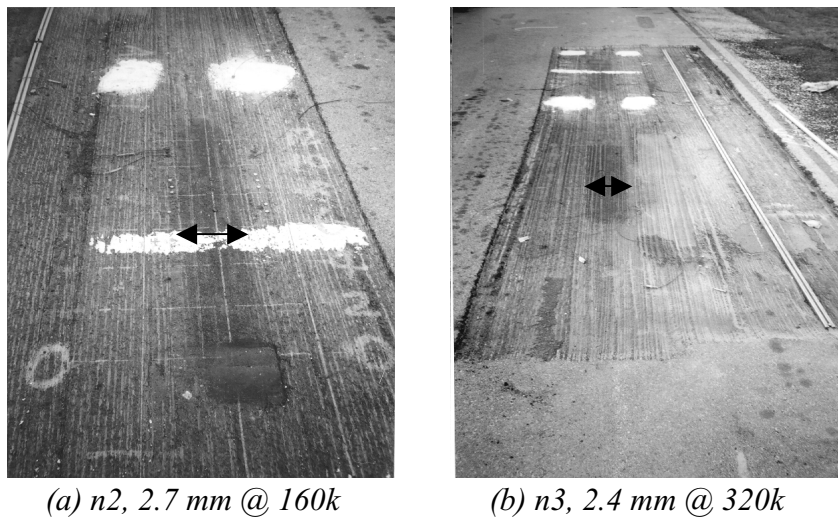
Figure 21: Surface ruts (n2 and n3)

The Southbound Lane (Pads s1, s2, and s3)

The ruts after 80k were 0.5 mm for s1, 1.25 mm for s2, and 0.9 mm for s3, respectively. After 160k, the rut depth on s1 was 0.6 mm and the depth on s3 was 1.1 mm. The new Remixer overlay (s1) appeared to have been more resistant to permanent deformation and less sensitive to temperature than the second layer of Remixer (s2). The higher rutting on s3 with respect to s1 at 160k suggests that the Remixer and the in-situ

LWAC are susceptible to water damage. As in the case of the northbound n3, the higher tire pressure on pad s3 would have affected the rutting, but no correction was made.

The Northbound (Dustrol) and Southbound (Remixer) Lanes

On average, the northbound lane had rutted about 2 times more than the southbound lane. The maximum n1 rut after 320k axles was 2.1 mm, and the 320k extrapolated s1 rut was about 0.8 mm. Similar conditions were present during testing on the two test pads. The maximum rut of s1 at the termination of testing at 180k was 0.6 mm, and the rut for n1 was about 1.5 mm. The rutting trend was the same in both cases (Figure 16). However, n1 had rutted about 2.8 times more than s1. Figure 22 shows the n1 and s1 rut profiles. The figure clearly shows the increased rutting of n1 and the coarse surface texture of the southbound structure (s1) that perhaps contributed to its resistance to rutting.

(a) n1, 2.2 mm @ 320k   *(b) s1, 0.6 mm @ 180k*

Figure 22: Surface ruts (n1 and s1)

The n2 maximum rut after 160k was 2.7 mm, and the s2 160k extrapolated rut was about 1.6 mm (Figure 17). The n2 ruts were higher than those on s2 at all axle counts. After 80k, the rut depth on n2 was 2.1 mm and on s2 was 1.3 mm. On average, n2 had rutted about 1.7 times more than s2.

As previously shown in Figure 18, the n3 maximum rut after 320k was 2.4 mm, and on s3 the rut depth was about 1.4 mm (extrapolated). Pad n3 rutted about 1.7 times more than s3. The increased rutting experienced on the wet tests was probably due to the increased tire pressure and distress resulting from water pressure on the LWAC.

Overall, the increased rutting of the milled pads compared to the surface tests was due to the increased temperature deeper within the pavement structures, as well as to water

damage (in the wet tests). Generally, the Remixer process on the southbound structure performed more rigidly and had a better surface rut performance than the Dustrol process on the northbound structure. This is an indication that the Dustrol process was more sensitive to temperature and moisture damage than the Remixer.

1998 and 1999 MMLS3 Rutting

Figure 19 showed the plot of the n-dry rut profiles for the 1998 MMLS3 dry test (no temperature control) and the 1999 MMLS3 hot tests. At 320k, the 1999 MMLS3-n1 rut was 2.2 mm, and the 1998 MMLS3 (n-dry) rut was 1.4 mm. The hot test rutting was about 60% greater than that in the 1998 dry test. At the termination of the 1998 dry test at 1.0 million axles, the rut was only 1.8 mm (about 83% of the hot test rut at 320k).

The average MMLS3 trafficking temperature at the 25 mm depth was 49.8 $^{\circ}$C for n1 (1999) and 37.9 $^{\circ}$C for n-dry (1998), a difference of about 12 $^{\circ}$C. Since the MMLS3 traffic loading was similar (2.1kN) in both cases, the high n1 (1999) rutting resulted from the increased temperature and contact pressure differential. This finding should correlate with the G* (shear stiffness) values of the layer at these two temperatures, provided the tire-pressure difference is also taken into account. This analysis is subsequently considered in the discussion of results.

On the other hand, n-wet (1998) at 24 $^{\circ}$C rutted about one third the amount measured on n1 (1999) at 320k (0.7 mm versus 2.2 mm). This finding is indicative of the marked influence of temperature on the performance of the upper layers. The rut depth on n-wet (1998) was only 1.0 mm at the termination of testing after 1.4 million axle loads compared to 2.4 mm for n3 (1999 milled wet) at 320k. This finding suggests that the recycled LWAC (Dustrol) was more sensitive to moisture than the top limestone AC surfacing layer.

TxMLS and MMLS3 Rutting

The comparative rut profiles were shown in Figure 20. For the TxMLS, only the surface ruts up to a depth of 90 mm were considered. After 320k axles, the one-third (1/3) scale MMLS3 rutting (n1 [1999]) was about one third of the full-scale TxMLS (2.17 mm versus 6.5 mm). The n-dry (1998) rut was 1.35 mm, compared with the TxMLS rut of 6.5 mm at 320k. This measure was only about 21% of the full-scale TxMLS rut. On pad n2, the rutting was 2.69 mm at 160k, which is 67% of the 4 mm TxMLS rut at the same axle count. Among other differences, there was no environmental control in the full-scale TxMLS trafficking or in the 1998 MMLS3 dry tests. Furthermore, the TxMLS traffic loading is much higher than the MMLS3, and naturally more rutting was to be expected. By contrast, there was more surface rutting on the southbound sections under the milled pads s2 and s3 than in the tests conducted with the TxMLS, which presumably had higher rutting in the lower layers (most probably in the base and subgrade).

Pads n2 and s2 yielded a better rut comparison owing to the milling effect, which resulted in high stresses being induced deeper down in the pavement layers; this effect to some extent simulated the TxMLS loading profile.

The main difference between the latest MMLS3 test program and the previous trafficking (TxMLS and MMLS3-1998) tests at Jacksboro was the environmental control.

3. Pavement Layer Deformation

The relative deformation of the pavement layers with MMLS3 trafficking was monitored using the small LDPs. The respective pavement layer deformations are shown in Table 4.

Table 4: Pavement layer deformations

		n1 [320k]		n2 [160k]		n3 [320k]	
(a) Northbound lane							
Thickness (mm)	**Layer**	**Def. (mm)**	**% age**	**Def. (mm)**	**% age**	**Def. (mm)**	**% age**
25	New limestone AC (1996)	1.06	49	Top layer milled off			
25	Recycled LWAC + Reclamite (Dustrol, 1996)	0.53	24	2.36	88	1.96	83
20	In situ LWAC (1986)	0.22	10	0.18	7	0.19	8
Below 70	Old AC layers, seal coat, base, and subgrade	0.36	17	0.15	5	0.20	9
Total		**~2.2**	**100**	**~2.7**	**100**	**~2.4**	**100**
(b) Southbound lane							
		s1 [180k]		s2 [80k]		s3 [160k]	
25	Recycled Top LWAC + limestone AC (Remixer, 1995)	0.23	36	Top layer milled off			
25/10	Recycled Bottom LWAC + limestone AC (Remixer, 1995)	0.17	27	0.64	51	0.45	42
20	In situ LWAC (1986)	0.11	17	0.43	34	0.41	38
Below 70	Old AC, seal coat, base, and subgrade	0.13	20	0.18	15	0.22	20
Total		**~0.6**	**100**	**~1.3**	**100**	**~1.1**	**100**
Key: Def. = Deformation, % age = Percentage contribution to total deformation							

The Northbound Lane

The total n1 rut after 320k was 2.2 mm, of which 49% occurred in the top 25 mm limestone AC layer. Some 24% occurred in the 25 mm recycled LWAC (Dustrol) and 10% in the 20 mm LWAC layer. A 17% deformation occurred in layers below the in-situ LWAC.

After 160k, n2 had rutted about 2.7 mm. About 88% occurred in the Dustrol processed layer (0–25 mm) and was probably due to the direct heating effect and MMLS3 trafficking after the protective limestone AC surfacing layer was milled off. Approximately 7% deformation occurred in the in-situ LWAC layer and the rest in underlying layers.

Eighty-three percent of the 2.4 mm total rutting of pad n3 at 320k axles occurred in the Dustrol layer (~25 mm recycled LWAC plus Reclamite). This effect was probably due to degradation and stripping of the LWAC as a result of water application on the surface. The rest (17%) occurred in underlying layers, with about 8% occurring in the 20 mm in-situ LWAC layer.

The Southbound Lane

On pad s1, about 63% deformation occurred in the top 50 mm of recycled LWAC (Remixer), and about 17% occurred in the in-situ LWAC layer. Approximately 20% deformation occurred in layers below the in-situ LWAC. The s1 total permanent deformation after 180k axles was 0.6 mm.

Pad s2 rutted about 1.3 mm after 80k axles. About 51% occurred in the bottom Remixer layer, which was directly exposed to MMLS3 trafficking and heating after the top 40 mm rehabilitation layer was milled off. The bottom layers contributed about 49%, with 34% occurring in the in-situ LWAC.

Of the 1.1 mm rutting of pad s3, about 42% deformation occurred in the top 10 mm second Remixer layer, which was undergoing stripping and degradation owing to the effects of water. About 38% deformation occurred in the in-situ LWAC and 20% in underlying layers. This effect was probably a result of water damage.

4. Microcracking and Stripping

Rutting, surface microcracking, and stripping were the anticipated modes of distress on the wet tests. Surface cracks were monitored prior to and at the termination of trafficking. Small microcracks were found on the n3 and s3 test pads after termination of the tests. In addition, after MMLS3 trafficking there were small, loose aggregate particles on the surface of the wet test pads as a result of stripping. Stripping was also evident on the wet pads at the lower interface of L3 and the 1971 AC, particularly on n3. No surface cracking was found on the hot test pads.

It was concluded that the surface cracking and stripping of the wet test pads was most probably due to degradation of the surface of the asphalt concrete by the effects of water. The microcracks were more prominent in n3 than in s3. .

Clear evidence of stripping was found during coring of the 1998 wet test section. The bond between Layer 3, the LWAC, and the AC below was much weaker in the trafficked cores than in the untrafficked ones. In some cases, there was no bond at all. The aggregate at the interface was also washed clean, indicative of stripping.

5. The Pavement In Situ AC Stiffness

The change in Young's moduli of the asphalt concrete surface layers for both the hot and wet tests owing to trafficking was monitored using the PSPA and SASW devices at selected points on the test pads. The pavement stiffness is related to the velocity of wave travel through the pavement and is strongly influenced by the pavement temperature at the time of the measurement. Accordingly, the results were normalized to standard temperatures of 25 °C (PSPA) and 21 °C (SASW), respectively (Li et al. 1994 and Aoud et al. 1993). These values are the standards selected by the original proponents of the respective devices, and in this research, no attempt was made to adjust these values. This lack of adjustment does not cause any discrepancy in the analysis since no comparison is being made between the two systems (PSPA and SASW).

PSPA

Figure 23 shows a plot of the normalized PSPA moduli ratios relative to the untrafficked sections. The AC moduli were normalized to 25 °C and 30 Hz using the relationship proposed by Li and Nazarian for adjusting raw AC moduli measured at a temperature T in degrees Celsius to a reference temperature of 25 °C (Li et al. 1994 and Aoud et al. 1993). The calculations were based on an average pavement AC density of 2,000 kg/m^3 and Poisson's ratio of 0.33.
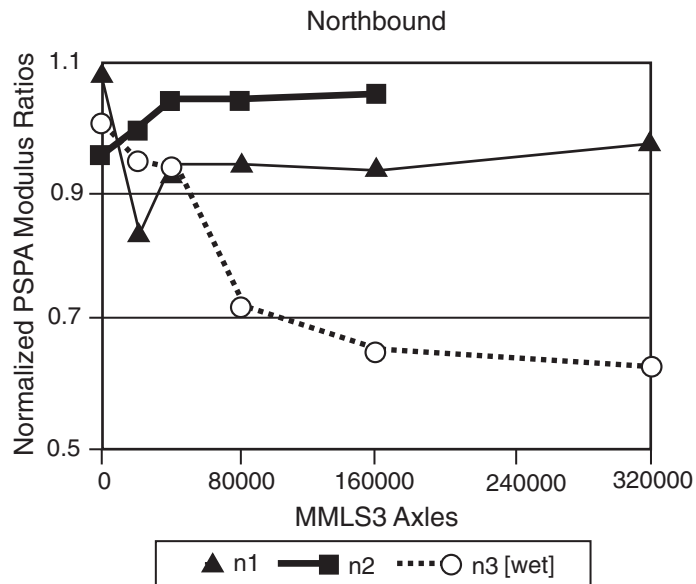
Figure 23 (a):   Normalized PSPA moduli (25 °C, 30 Hz)
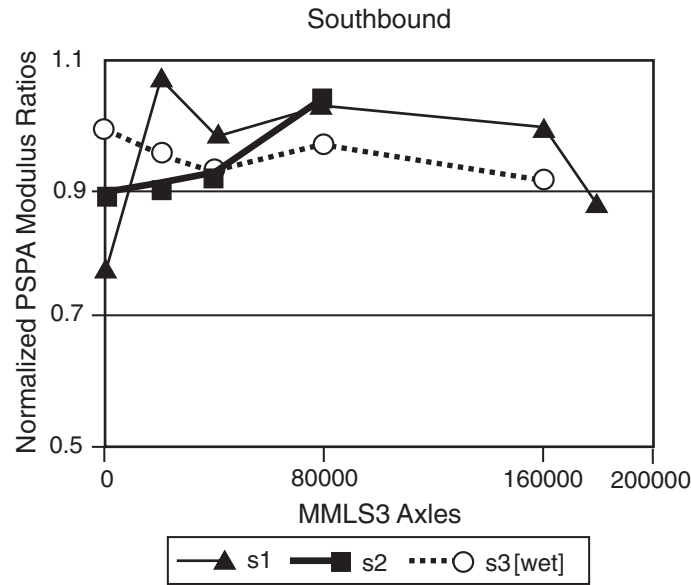
Figure 23 (b): Normalized PSPA moduli (25 °C, 30 Hz)

Figure 23 shows that there was a decrease in pavement AC moduli in pads n1, n3, and s3 with MMLS3 trafficking. In pads s1, n2, and s2 there was an increase. As a result of anticipated traffic damage, the moduli would normally be expected to decrease with trafficking. However, material densification resulting from traffic may offset the effects of traffic damage, as was evident in pads s1, n2, and s2. Tangella (1990) and Raithby and Ramshaw (1972) have also reported this phenomenon.

The decrease in AC pavement moduli on both the wet tests (n3 and s3) suggests water damage (AC degradation and stripping). There was a loss in stiffness of about 37% in the northbound structure and about 8% in the southbound structure owing to MMLS3 trafficking in the presence of water.

In comparative terms, the average PSPA moduli for the southbound pavement structure (~3 550MPa) were about 17% higher than the northbound (~3 035MPa). This finding compares favorably with Hugo's findings that the 281S1 average modulus was approximately 20% higher than the 281N1 (Hugo et al. 1999). Lee et al. (1997) found similar results. This finding partially explains the higher resistance to deformation and the smaller ruts obtained on the southbound lane during MMLS3 trafficking.

SASW

Table 5 shows the normalized SASW moduli ratios. The SASW measurements were made after the tests were completed. Analysis was based on a comparison with control measurements from the untrafficked sections.

The raw moduli were calculated from the SASW surface-wave velocity. The calculation was based on the linear-elastic relationship between the shear and Young's modulus of elasticity and on the assumption that the surface-wave velocity was about 90% of the shear-wave velocity (Aoud 1993). An average AC pavement density of 2,000 kg/m^3 and Poisson's ratio of 0.33 were also assumed. The raw moduli were normalized to 30 Hz frequency and 21 $^\circ$C using the correction equations developed by Aoud (1993).

The SASW normalized moduli ratios in Table 5 show that there was a significant drop in stiffness in the wet pads n3 (~33%) and s3 (~11%). In addition, the trafficked moduli for the wet pads were of a magnitude lower than that of the hot pads. This finding correlates well with the PSPA results, and the loss in stiffness appears to be primarily due to water.

The results indicated that there was no significant change in modulus in pad n1. However, pad s1 appeared to have gained stiffness on the order of about 15% owing to MMLS3 compaction. This stiffness gain is indicative of the difference between the performances of the limestone and the LWAC, as is discussed later.

Table 5: Normalized SASW AC moduli (MPa) ratios after MMLS3 trafficking

Normalized Pavement AC Moduli Ratio to 21°C, 30 Hz			
Pad	SASW Modulus Ratio (relative to untrafficked sections)	Test Type	Comment
n1	0.99	Dry-hot	-1%
n2	1.02	Dry-hot	+2%
n3	0.67	Wet	**33% loss**
s1	1.15	Dry-hot	15% gain
s2	1.02	Dry-hot	+2%
s3	0.89	Wet	**11% loss**

6. Laboratory Test Results

Volumetrics

Table 6 shows a general increase in bulk specific gravity (BSG) after both trafficking and wetting. The increase in BSG was attributed to the decrease in voids resulting from densification under MMLS3 trafficking. However, there was a loss in relative density on the wet pads (Table 7) of about 4% on the northbound structure and 2% on the southbound structure owing to stripping.

The measured air voids and voids in the mineral aggregate (VMA) from the northbound untrafficked sections were 8.6% and 20.1% for the composite specimens, and 9.3% and 22.5% for the lightweight specimens, respectively. This high void content explains the high consolidation (i.e., about a 4% increase in BSG) and high rutting of the LWAC

(under hot MMLS3 trafficking) in comparison with the top limestone AC surfacing layer on the northbound structure.

Table 6: Material volumetrics

ID	Type	Section	MMLS3 trafficking	2 hrs wet conditioned	Diameter (mm)	Thickness (mm)	BSG	Density (kg/m3)	Change in BSG (%)
					(a) Northbound				
5	L1	nu	no	no	101.60	24.68	2.20	2,198.25	
2	L1	nu	no	yes	101.60	18.95	2.23	2,225.50	
5	L2	nu	no	no	101.60	25.30	1.66	1,660.80	
2	L2	nu	no	yes	101.60	25.10	1.71	1,712.50	+3.01
4	L1	n1	yes	no	101.60	27.00	2.26	2,258.50	+2.67
4	L2	n1	yes	no	101.60	26.25	1.77	1,766.50	+5.98
4	L2	n2	yes	no	101.60	27.25	1.74	1,736.00	+4.33
4	L2	n3	yes	no	101.60	26.00	1.66	1,658.50	-0.10
					(b) Southbound				
2	L1	su	no	no	101.60	28.75	1.97	1,968.00	
4	L1	su	no	yes	101.60	27.00	1.90	1,898.00	-3.55
2	L2	su	no	no	101.60	28.80	1.71	1,712.00	
4	L2	su	no	yes	101.60	25.95	1.72	1,723.00	+0.64
4	L1	s1	yes	no	101.60	27.25	1.904	1,903.50	-3.28
4	L2	s1	yes	no	101.60	26.95	1.68	1,680.00	-1.87
4	L2	s2	yes	no	101.60	16.10	1.75	1,749.52	+2.39
4	L2	s3	yes	no	101.60	23.75	1.72	1,717.00	+0.29
L13	L*	North	no	no	152.40	44.50	1.68	1,680.00	
L16	L*	North	no	yes	152.40	45.65	1.68	1,681.00	+0.06
W6	L*	Wet	yes	no	152.40	51.33	1.66	1,662.00	
W4	L*	Wet	yes	yes	152.40	56.10	1.73	1,731.00	+4.15
D3	L*	Dry	yes	yes	152.40	53.90	1.69	1,694.00	
12	C	North	no	no	152.40	49.75	2.03	2,026.50	
8	C	North	no	yes	152.40	49.65	2.03	2,034.00	+0.39

Table 7(a): Summary of lab test results for northbound inner lane

Core Details	Test	nu Result	nu RR	n1 Result	n1 RR	n2 Result	n2 RR	n3 Result	n3 RR	nw Result	nw RR	nu-D Result	nu-D RR	nd Result	nd RR
Layer 1 / Limestone AC / ~25 mm (nu-D,nd: ~15 mm)	ITS [20 °C, 50 mm/min] (kPa)	1076/1202*	1	749	0.62					1399	1.16	752	1	972	1.29
	SCB [20 °C, 5 mm/min] (MPa)	2.45	1	2.5	1.02					2.72	1.11	1.26	1	2	1.59
	Relative Density	2.153	1	2.258	1.05					2.353	1.09	2.16	1	2.205	1.02
	Fatigue Life [20% 1076 kPa, 20 °C, 10 Hz]	884 800	1	1 519 800	1.70					785 533	0.89	271 375	1	311 345	1.15
Layer 2 / Dustrol / ~25 mm	ITS [20 °C, 50 mm/min] (kPa)	714/894*	1	1131	1.27	1089	1.22	991	1.11	977	1.09	597	1	825	1.38
	SCB [20 °C, 5 mm/min] (MPa)	2.035	1	2.09	1.03	2.05	1.01	1.69	0.83	1.72	0.85	1.14	1	1.29	1.13
	Relative Density	1.664	1	1.770	1.06	1.736	1.04	1.605	0.96	1.653	0.99	1.718	1	1.685	0.98
	Fatigue Life [20% 842 kPa, 20 °C, 10 Hz]	855 000	1	901 500	1.05	1 125 600	1.32	488 600	0.57	186 437	0.22	268 815	1	277 225	1.03
Layer3 / In situ LWAC / ~20 mm	ITS [20 °C, 50 mm/min] (kPa)	458	1									584	1		
	SCB [20 °C, 5 mm/min] (MPa)	1.95	1	1.96	1.01	1.86	0.95	1.18	0.61	1.28	0.66	0.938	1	1.615	1.72
	Relative Density	1.659	1	1.664	1.00	1.668	1.01	1.645	0.99	1.661	1.00	1.673	1	1.67	1.00
	Fatigue Life [20% 458 kPa, 20 °C, 10 Hz]	859 880	1	936 000	1.09	742 680	0.86	340 000	0.40	171 420	0.20	235 365	1	336 850	1.43
	MMLS3 Axle Loads	none		320 000		160 000		320 000		1 400 000		none		1 000 000	
	MMLS3 Trafficking Temperature (°C)	none		50		50		30		24		none		38	
	MMLS3 Trafficking Condition	none		Hot (heated)		Hot (heated)		Wet (1mm water)		Wet (1 mm water)		none		Dry	

Key: AC = Asphalt Concrete, LWAC = Lightweight Aggregate (Asphalt) Concrete, RR = Relative Ratio to Untrafficked Section (nu),

ITS = Indirect Tensile Strength, SCB = Tensile Stresses in Semicircular Bending Test

33

Table 7(b): Summary of lab test results for southbound inner lane

Core Details			Test	su		s1		s2		s3	
				Result	RR	Result	RR	Result	RR	Result	RR
Layer 1	Top Remixer	~25 mm	ITS [20 °C, 50 mm/min] (kPa)	1153/1128*	1	1320*	1.17				
			SCB [20 °C, 5 mm/min] (MPa)	2.33	1	2.53	1.09				
			Relative Density	1.961	1	1.984	1.01				
			Fatigue Life [20% 1128 kPa, 20 °C, 10 Hz]	892 743	1	1 150 000	1.29				
Layer 2	Bottom Remixer	~20 mm	ITS [20 °C, 50 mm/min] (kPa)	1026/1142*	1	1083*	0.95	875*	0.77	1044*	0.91
			SCB [20 °C, 5 mm/min] (MPa)	2.07	1	2.08	1.05	1.85	0.89	1.93	0.93
			Relative Density	1.712	1	1.724	1.01	1.749	1.02	1.686	0.98
			Fatigue Life [20% 1142 kPa, 20 °C, 10 Hz]	398 405	1	425 600	1.07	472 050	1.18	358 200	0.90
Layer3	In situ LWAC	~20 mm	ITS [20 °C, 50 mm/min] (kPa)	802	1						
			SCB [20 °C, 5 mm/min] (MPa)	1.91	1	1.93	1.01	1.95	1.02	1.65	0.86
			Relative Density	1.616	1	1.68	1.04	1.680	1.04	1.656	1.02
			Fatigue Life [20% 458 kPa, 20 °C, 10 Hz]	733 785	1	752 400	1.03	802 000	1.09	512 600	0.70
MMLS3 Axle Loads				none		180 000		80 000		160 000	
MMLS3 Trafficking Temperature (°C)				none		50		50		30	
MMLS3 Trafficking Condition				none		Hot (heated)		Hot (heated)		Wet (1mm water)	

Key: AC = Asphalt Concrete, LWAC = Lightweight Aggregate (Asphalt) Concrete, RR = Relative Ratio to Untrafficked Section (su), ITS = Indirect Tensile Strength, SCB = Tensile Stresses in Semi-Circular Bending Test

34

Moisture Sensitivity

Table 8 shows the average moisture sensitivity test results for specimens cut from both the northbound and southbound cores. The low retained tensile-strength ratio (TSR = 0.57) for the northbound surface (S) specimens before trafficking correlated with the results from the larger specimens (Smit et al. 1999) and again suggests that the surface layer was moisture sensitive. The TSR values for the southbound structure before trafficking indicate that the surface (LWAC) layer is not moisture-susceptible (TSR = 0.91) but that the underlying second Remixer layer may be moisture-susceptible (TSR = 0.81). The results also show that the top two layers in the southbound structure, both LWAC, have approximately the same indirect tensile strengths. These two layers constitute the Remixer process. Both of these layers are stronger than the recycled LWAC Dustrol layer in the northbound structure.

Table 8: Moisture sensitivity results at 25 °C (AASHTO T283)

Type	Section	MMLS3 trafficking	2 hrs wet conditioning	Diameter (mm)	Thickness (mm)	No. of Specimens	ITS Strength (kPa)	RTSR	Failure Strain
(a) Northbound									
L1	nu	no	no	100	25	4	1 202		0.0027
L1	nu	no	yes	100	19	2	679	0.57	0.0036
L2	nu	no	no	100	25	5	894		0.0046
L2	nu	no	yes	100	25	2	760	0.85	0.0057
(b) Southbound									
L1	su	no	no	100	28.8	2	1 128		0.0056
L1	su	no	yes	100	27.0	2	1 025	0.91	0.0043
L2	su	no	no	100	28.8	2	1 142		0.0043
L2	su	no	yes	100	26.0	2	923	0.81	0.0045

Key: RTSR — Retained tensile strength ratio.

From the above results, the research team concluded that meeting the T283 specifications does not necessarily mean that the AC will not be damaged by water or will not strip. Likewise, failure to meet the specification (TSR≥0.8) may not necessarily mean that the AC will be damaged by water or will strip.

Shear Testing

Shear frequency sweeps were conducted at 25 °C and 40 °C for composite (C) specimens and at 40 °C for lightweight (L) specimens. Table 9 presents the average shear frequency sweep data for the larger composite (C) and lightweight (L) specimens from the northbound pavement structure. The respective values for the loading frequencies of the

TxMLS (3 Hz) and the MMLS3 (4 Hz) were interpolated. These results compare favorably with those reported by Hugo et al. (1999).

Table 9: Average SST frequency sweep results for the northbound pavement structure

Section	Specimen	Test Temperature (°C)	Test Frequency (Hz)	Shear Modulus G* (kPa)	Elastic Modulus E (MPa)	Phase Angle (δ)	Comment
Nu	Composite	40	2	2.69 E05	715.54	42.1	
			3	3.27 E05	870	41.0	interpolated
			4	3.76 E05	1 000	40.2	interpolated
			5	4.13 E05	1 098.58	39.9	
			10	5.34 E05	1 420.44	43.3	
Nu	Lightweight	40	2	2.41 E05	641.06	41.6	
			3	2.89 E05	770	40.5	interpolated
			4	3.32 E05	885	39.4	interpolated
			5	3.67 E05	976.22	39.1	
			10	4.67 E05	1 242.22	41.6	
Nu	Composite	25	2	10.26 E05	2 729.16	24.2	
			3	10.90 E05	2 900	24.5	interpolated
			4	11.56 E05	3 075	25.0	interpolated
			5	12.02 E05	3 197.32	25.6	
			10	13.40 E05	3 564.40	29.5	

The results indicate that the upper surface layers and the underlying lightweight layer could be expected to behave more rigidly (with a greater stiffness) under the MMLS3 (4 Hz) than they would under the TxMLS (3 Hz). This effect of loading time shows why there was substantial resistance to permanent deformation in the pavement surface layers. With the MMLS3 influencing only the surface layers, this result partially explains the small rut depths measured in the 1998 MMLS3 tests by Smit et al. (1999).

By comparison, the two types of specimens showed only appreciable differences in shear stiffness (G*), with higher values for the composite (C) specimens at both representative frequencies. In addition, at the lower testing temperature the composite (C) specimens exhibited more elastic behavior (lower phase angle [δ]) with higher shear stiffness (G*), as expected. Higher resistance to rutting was thus expected at low temperatures rather than at high temperatures. Furthermore, the high modulus value of the composite specimen compared to the lightweight specimen (at 40 °C) indicated that the limestone AC might be more resistant to rutting than the LWAC. This indication agrees with the n1 and n2 surface ruts measured at 50 °C.

ITS and SCB Test Results

The indirect tensile strengths (ITS) in axial mode indicated an increase of approximately 20% (Table 10) in strength for the Dustrol process on the northbound structure after MMLS3 trafficking relative to the virgin asphalt nu. The increase in strength was perhaps due to densification under MMLS3 trafficking, as was evident from the decrease in air voids and the increase in relative density (~4%). This finding partially explains the relatively high indirect tensile fatigue life obtained for pad n2, as is presented later. However, this does not account for the microcracking and stripping or the loss in stiffness on the wet pad n3. A decrease of about 38% in ITS strength was observed for the top limestone AC. The semicircular bending (SCB) test results (Table 7 [a]) indicated an increase in strength for n1 and n2 and a decrease of about 17% for n3 (wet test).

Table 10: ITS strength ratios and change in ductility at 25 $^{\circ}$C

Section	Specimen Type	Layer No.	ITS Strength Ratio (relative to untrafficked sections)	Strain ($\Delta\varepsilon_f$)	Comment
n1	Surface	1	0.62	$-0.6 * 10^{-3}$	38% loss
n1	Lightweight	2	1.27	$0.8 * 10^{-3}$	27% gain
n2	Lightweight	2	1.22	$-1.3 * 10^{-3}$	22% gain
n3	Lightweight	2	1.11	$-1.7 * 10^{-3}$	11% gain
s1	Surface	1	1.17	$-1.9 * 10^{-3}$	17% gain
s1	Lightweight	2	0.95	$-0.2 * 10^{-3}$	05% loss
s2	Lightweight	2	0.77	$-0.8 * 10^{-3}$	23% loss
s3	Lightweight	2	0.91	$-1.4 * 10^{-3}$	**09% loss**

In the southbound section, there was a decrease in both ITS (~9%) and SCB (~7%) strength on the wet test pad s3 (Tables 7[b] and 10). The strength loss was attributed to the effects of water. A decrease in strength was also evident for all the other sections and layers, except s1 layer 1 (the new Remixer overlay), which had indicated an increase of about 17% in ITS strength. Densification resulting from MMLS3 traffic consolidation was the probable cause.

There was an average decrease of 9% to 43% in ITS strength in all specimens after wetting (Table 8). This strength decrease is an indication that the pavement layers were sensitive to moisture. Table 8 also shows that with the exception of the surface layer, the ITS values for the southbound layers were relatively higher than those from the northbound structure.

ITS Strength Ratios

Table 7 presented the ITS strength results as ratios of the trafficked specimens (n1, n2, n3, s1, s2, and s3) to respective untrafficked specimens nu and su. A loss of strength with trafficking is shown for the n1 surface layer, the s1 lightweight layer, the s2 lightweight layer, which was directly beneath the MMLS3 after milling, and the s3 lightweight layer, which was also directly beneath the MMLS3 after milling. The indication of damage caused by trafficking for the n1 surface layer but not for the s1 surface layer correlates with the TSR results indicating moisture susceptibility for the same n1 limestone AC surface layer. This finding also agrees with the PSPA and SASW results. A gradual decrease in ITS strength ratio is also shown for the northbound sections, with the highest ratio for the n1 lightweight Dustrol layer followed by those for the unprotected n2 and n3 (wet). As expected, after the surface layer was milled off, the unprotected s2 and s3 lightweight layers exhibited a greater loss of strength than did the protected s1 lightweight layer. Because of the presence of water throughout the s3 test, the ITS strength ratio for the s3 lightweight (L) layer was expected to be lower than the ratio for the s2 lightweight (L) layer.

Indirect Tensile Fatigue

The indirect tensile fatigue test results presented in Table 7 are from the three topmost layers of the northbound and southbound pavement structures, respectively. These tests were done at a loading frequency of 10 Hz and 20 $^{\circ}$C with no rest periods. The loads were set at 20% of the respective ITS values and at 90° to the direction of MMLS3 trafficking.

The results show that the heated asphalt layers (pads n1, n2, s1, and s2) gained fatigue life on the order of about 20% for the northbound and 13% for the southbound structures, because of MMLS3 traffic compaction. J. Epps (1969), Tangella (1990), and Raithby and Ramshaw (1972) had also found that traffic compaction and an increase in asphalt stiffness increased fatigue life to the extent that it offset the effects of damage caused by traffic. However, the fatigue life subsequently decreases with extended trafficking owing to damage.

The wet pads showed a reduction in fatigue life relative to the virgin asphalt as well as in comparison with the heated pads n1, n2, s1, and s2. Figure 24 shows these results graphically. The Dustrol on pad n3 had a reduction of about 43% (after 320k), while the reduction for the bottom Remixer on pad s3 was about 10% (after 160k). These reductions were due to the damaging effects of water. The LWAC on the southbound section had a loss of about 30% after 160k, and the northbound had a loss of 60% for the LWAC after 320k. Figure 24 shows that these changes fall on the same line and thus exhibit a degree and extent of water damage similar to the amount they would have exhibited had they been subjected to the same number of MMLS3 traffic axles. This finding was not surprising since it is virtually the same material. The damage under extended trafficking for both the Dustrol and LWAC was far greater, as evident from the 21% residual fatigue life of nw after 1.4 million load applications (Table 7[a] and Figure 24). However, the slope of the 1998 Dustrol and LWAC graphs (Figure 24) is not as steep as that of the corresponding 1999 graphs. This difference is

an indication that the progression of water damage was not as rapid and as intensive as that in the 1999 wet tests owing to the limestone AC cover in the 1998 test. It should be remembered that the top 25 mm of limestone AC was milled off in the 1999 wet tests. If MMLS3 trafficking had continued in the 1999 wet tests, the bottom Remixer, the Dustrol, and the in situ LWAC would have been reduced to about 21% residual fatigue life after about 1,226k, 585k, and 455k, respectively. The damaging effect of wet axles is apparent, and it is clear that the number of axle loads that can be carried is significantly reduced under wet conditions, even under the light wheel loads of the MMLS3. In fact, because the south- and northbound LWACs (L3) were found to be equally susceptible to water damage, both pavement structures would probably perform the same under wet trafficking, especially if water could gain access to the LWAC layer through cracks or through a porous surface.
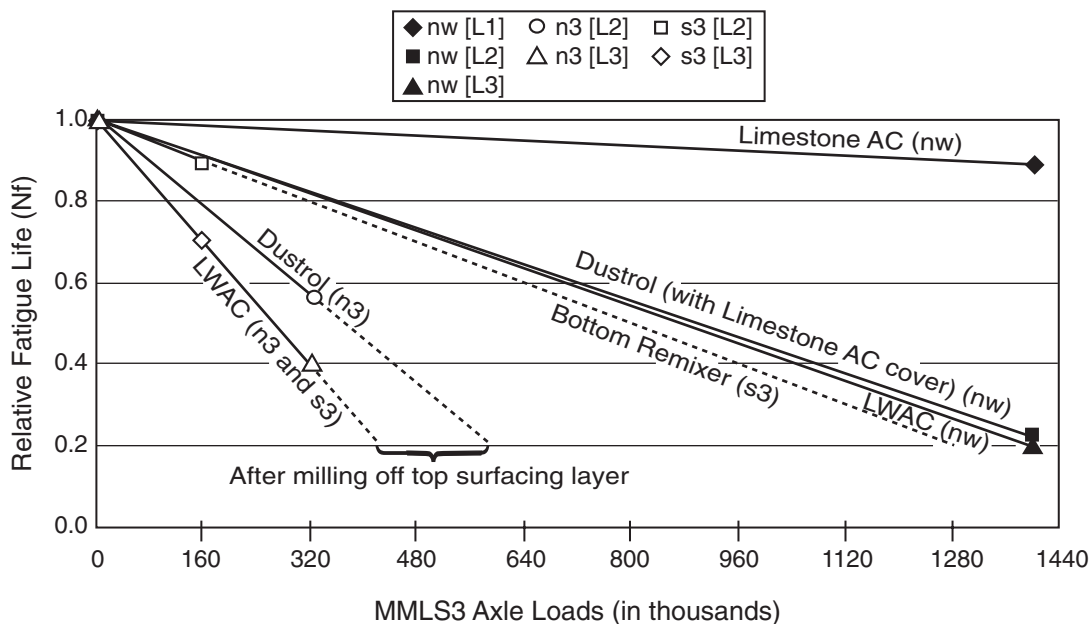
Figure 24: Relative indirect tensile fatigue life (Nf) after MMLS3 wet trafficking

Both Table 7[a] and Figure 24 indicate that the upper limestone AC on the northbound structure appeared to be less affected by water; it had a residual fatigue life of about 89% of the original asphalt after 1.4 million MMLS3 axle loads. This finding is contrary to the prediction in terms of the American Association of State Highway and Transportation Officials (AASHTO) T283 test results.

Relatively shorter fatigue lives were obtained from the nd section (Smit et al. 1999) on both the untrafficked and trafficked cores. This finding was ascribed to the poorer material in this section, as was discussed previously. However, the relative ratio (RR) of the

fatigue life (with respect to the untrafficked section nu-D) of the limestone AC (layer 1) and Dustrol (layer 2) for the nd section (Table 7[a]) exhibited a trend similar to the results for pads n1 and n2, albeit their N_f values were of smaller magnitude. This trend is indicative of the damage from extended trafficking (1.0 million axle loads) and the effect of temperature.

Overall, the Dustrol in the hot, dry trafficked test sections had a better indirect tensile fatigue performance (in terms of the number of fatigue load cycles to crack failure) than the Remixer.

7. Stress Analysis

To check the measured deformation values and to compare the MMLS3-TxMLS stress profiles, the research team used the computer program BISAR 3.0 (Shell Bitumen, 1998) to compute the vertical stresses within the pavement layers, based on the material properties presented in Table 11. Assuming linear elastic behavior, all the pavement materials in Table 11 were characterized using Young's modulus of elasticity (E) and Poisson's ratio (ν). The respective AC moduli were reduced to the corresponding measured middepth layer temperatures (Figure 12) from 25 °C using the falling weight deflectometer (FWD) temperature-correction equations developed by Hugo et al. (1999) and the Young's modulus temperature-correction curves developed by Lee et al. (1997).

Table 11: Pavement structures and stiffness values

Pad	Layer	Thickness (mm)	25 °C	at 50 °C n1	s1	at 50 °C n2	s2	at 30 °C n3	s3
N	New Limestone AC (1996, 8.6%)	25	3500	1350					
	Recycled LWAC + Reclamite (Dustrol, 1996)	25	2200	1070		850		2000	
	In situ LWAC	20	2400	1400		1170		2270	
S	Recycled LWAC + Limestone AC (Top Remixer, 1995)	25	3500		1700				
	Recycled LWAC + Limestone AC (Bottom Remixer, 1995)	25/10	3500		1700		1400		3180
	In situ LWAC (1986)	20	2400		1390		1030		2080
Other Layers	Limestone AC (1976)	30	3500	2600	2230	1980	1900	3325	3100
	Composite Aggregate AC (Heavyweight + Lightweight, 1971)	40	2000	1740	1470	1380	1280	2000	1740
	Old AC	40	1500	1490	1270	1230	1070	1600	1400
	Seal Coat (1957)	15	800	800	800	700	620	880	780
	Base (1957)	380	400			Stiffness values are temperature insensitive			
	Subgrade	2000/1325	200						
	Bedrock		20000						
	Poisson's ratio: 0.35								

The loading configurations that were used in the BISAR 3.0 stress analysis were 2.1kN, 420kPa for the MMLS3; and 37.8kN dual tire load, 690kPa tire contact pressure for the TxMLS. In the case of the MMLS3, only the hot tests were considered. Vertical stress profiles were plotted as shown in Figure 25 for both the northbound and southbound pavement structures. The TxMLS stress distribution was deliberately truncated at about 175mm depth (Figure 25), as interest was only in the top AC layers. The TxMLS stress influence extends way deeper into the base and subgrade.
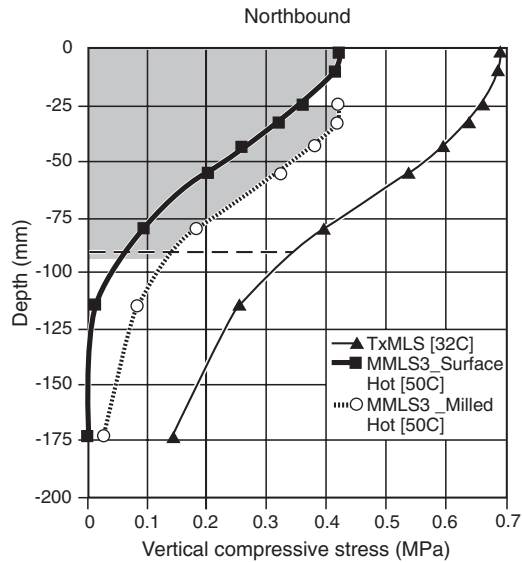

Figure 25(a): MMLS3-TxMLS vertical stress profiles (northbound)
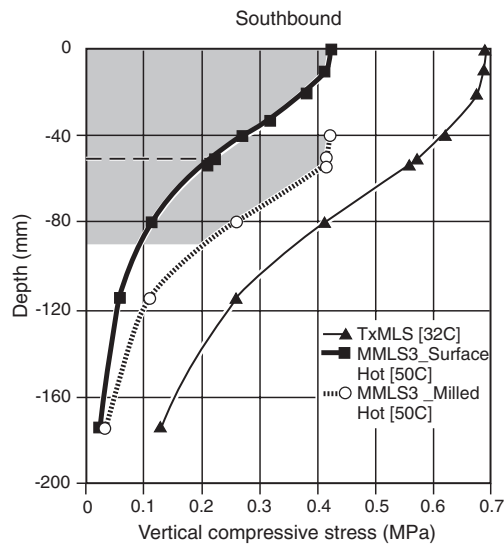

Figure 25(b): MMLS3-TxMLS vertical stress profiles (southbound)

The areas encompassed by the maximum vertical compressive stress distribution with depth for each loading condition (MMLS3, full-scale) are defined as corresponding rutting potentials (RPs) of a specific pavement section or layer. The rutting potential ratio (RPR) is calculated as the ratio of these RP values as follows:

$$RPR = RP_{MMLS3} / RP_{Full\text{-}Scale}$$

RPR based on the RPup to 90 mm in depth were computed and related to the measured permanent deformations as shown in Table 12. A planimeter was used to determine the areas within the stress bowls.

Table 12: Comparison of MMLS3-TxMLS rut ratios up to about 90 mm depth

Lane	Calculations		RPR	TCF	TRR	FRR	TRR versus FRR
	Permanent Deformation (mm)	**RP (MPa*mm)**					
North	**1**.MMLS3: n1 top 25 mm + n2 top 70 mm @ 320 = 1.1+ 3.7 ≈ 4.8 mm	MMLS3: 29.48	0.59	3.53	2.1	1.7	1.2
	2. Average TxMLS rut in top 90 mm @ 320k ≈ 2.9 mm	TxMLS: 50.14					
South	**1**.MMLS3: s1 top 50 mm + s2 top 50 mm @ 160k* = 0.4 + 1.4≈1.8 mm	MMLS3: 42.36	0.67	3.26	2.2	2.3	1.0
	2. Average TxMLS rut in top 90 mm @ 160k ≈ 0.8 mm	TxMLS: 63.28					

Key: RP = Rutting Potential, RPR= Rutting Potential Ratio, TCF = Temperature Correction Factor, TRR = Theoretical Rut Ratio, FRR = Field Rut Ratio

* Values obtained from extrapolated data shown in Figures 18 and 20.

DISCUSSION OF THE RESULTS

Temperature Profile

The temperature profile within the pavement structures was such that there was a gradual decrease in both temperature gradient and variation with depth, as shown in Figure 12. These temperatures were used in the analysis of the various test sections.

Comparison of Surface Ruts

The southbound lane had relatively smaller surface ruts than the northbound lane at the same axle loads and under different but similar environmental conditions. At 160k axle

loads, the n1 rut was 1.4mm, and the s1 rut was 0.62 mm. The new Remixer rehabilitation process (southbound lane) was more resistant to permanent deformation than the Dustrol rehabilitation process.

The comparative surface rut performance of n1 and n2 at 160k (1.4 mm against 2.7 mm) showed that the Dustrol process (lightweight AC in n2) was less resistant to deformation than the limestone AC surfacing layer. A similar trend was observed in the southbound lane when comparing s1 and s2 at 80k axle loads. Direct environmental exposure and, especially, heating were contributing factors to the increase in rutting in milled pads n2 and s2 compared with the surface rehabilitation processes. The marginally higher rut depths in the wet pads n3 and s3 indicate that water damage, degradation, and stripping of the LWAC may be as damaging as the heat, if not more damaging.

The substantially higher rut depths of the MMLS3 1999 northbound sections, compared with those of the MMLS3 1998 northbound sections, are attributed to the effects of temperature, as it was the primary variable condition. As expected, much deeper ruts were obtained under the TxMLS. However, a comparison based on the surface layer deformation (not the total rut) up to about 90 mm of depth demonstrated that the MMLS3 (milled test pads) and TxMLS permanent deformations were comparable within acceptable limits. In fact, the southbound milled pads had more surface deformations in the upper 90 mm layers than did the TxMLS. The trends in the two tests were similar. For example, the northbound lane had rutted more than the southbound lane in both cases.

In the case of the wet tests (30 C) n3 and s3, there was more deformation in s3 because of the LWAC. This may have been due to the fact that the L2 in s3 was thinner than the L2 in n3, and it therefore did not offer much protection against deformation in the lower in situ LWAC.

Comparison of Layer Deformation

Analysis of the LDP results for the northbound sections showed that a higher percentage of total permanent deformation occurred in the recycled LWAC (Dustrol) layer in n2 (88%) and n3 (83%) than in the limestone AC surfacing layer (49%). This finding demonstrates that the second Dustrol LWAC layer was relatively less resistant to permanent deformation and was more sensitive to temperature and moisture than the limestone AC overlay. On the southbound structure, the new Remixer rehabilitation process had deformed much less than the in situ LWAC but more than the limestone AC surfacing, indicating a higher resistance to permanent deformation than that of the Dustrol. The Remixer had behaved more rigidly than the Dustrol process.

Comparison with the Hamburg Test

A direct comparison between the Hamburg test results (Hugo et al. 1999) and the MMLS3 trafficking test results is difficult since the test methods are different in terms of temperature, stress, and load cycles. The Hamburg wheel-tracking device (HWTD) test is

empirical, whereas the MMLS3 provides performance results under pneumatic tires in a unidirectional trafficking mode at conventional tire pressure. In the case of the HWTD, the test specimens were 62 mm thick. They were cut from cores taken from the AC layer. Accordingly, the top specimen was composed of L1, L2, and part of L3. The bottom composite specimen (also 62 mm thick) consisted of the lower part of L3 and about 50 mm of AC material dating back to 1971.

The standard Hamburg test results of Hugo et al. (1999) are contained in Table 13[a] and show that the top composite layers of both the northbound and southbound sections performed similarly at 40 $^{\circ}$C and 50 $^{\circ}$C. The bottom composite layers indicated a significant difference in rut performance between the southbound and northbound sections at 40 $^{\circ}$C. However, at 50 $^{\circ}$C their respective performances were very similar, with the southbound specimens exhibiting marginally better performance.

Table 13: Rutting potential using the Hamburg wheel-tracking device (HWTD) (Hugo et al. 1999)

Layer	Temperature (°C)	Average Rut (mm)	
		281S	281N
(a) Rutting up to 20,000 standard passes			
Top 62 mm	40	2.04	02.15
	50	3.37	03.20
Bottom 62 mm	40	1.79	09.68
	50	12.30	15.18
(b) Rutting under nonstandard passes			
Top 62 mm	40	02.87 [99,900]	02.94 [99,000]
	50	16.67 [54,400]	19.42 [69,100]
Bottom 62 mm	40	19.00 [97,100]	14.39 [26,000]
	50	18.42 [30,200]	15.18 [17,800]

Hugo et al. (1999) also reported results from HWTD tests that were conducted in a nonstandard fashion (Table 13[b]). Trafficking was continued until the maximum rut capacity of about 20 mm was reached. Once again, the top composite layers showed no difference in rut performance at 40 $^{\circ}$C and 50 $^{\circ}$C. In the bottom composite layers, the northbound section was much more prone to rutting, i.e., it was susceptible to damage at temperatures of 40 $^{\circ}$C. At 50 $^{\circ}$C, the northbound rutting was about 1.5 times that of the southbound.

In the case of the MMLS3 it should be remembered that the tire pressures for tests n1, n2, s1 and s2 were only 420 kPa in contrast to tests n3 and s3 where the pressures were 690 kPa. Nevertheless, all three northbound test pads had greater deformation than the

southbound test pads. Details are given in Table 4. When the performance of the different layers is considered, L1 and L2 in pad n1 had about 2.5 times the rut depth of L1 and L2 in pad s1 at equivalent axle loads. From this, it is clear that the MMLS3 showed the northbound section to be more rut susceptible than the southbound section for the upper two layers. This is contrary to the results obtained from the Hamburg test.

When the deformation of the L3 layers is considered for the n1 and s1 tests, the northbound sections again had more deformation than the southbound ones (about 1.5 times). If the deformation below L3 is included, the composite deformation of the northbound test pads exhibits a similar trend. Therefore, these results are similar to those found with the HWTD test at 50 °C.

In terms of temperature susceptibility, the MMLS3 showed L2 to be more temperature susceptible in both the northbound and southbound sections. The results of the Hamburg test did not detect this.

Overall, both the MMLS3 and the HWTD indicated high rut potential for the northbound compared to the southbound pavement structure.

However, the results of the Hamburg test were in some instances contrary to the actual performance under MMLS3 trafficking. Based on the fact that MMLS3 trafficking closely simulates real traffic with pneumatic tires, it was concluded that the Hamburg test may have limitations and therefore further comparative studies are needed.

MMLS3 versus TxMLS Rutting Performance

The rutting performance of the MMLS3 was compared to that of the TxMLS by taking account of temperature differences as well as the tire pressures and RPRs. The comparison was based on the theoretical and actual field rut ratios. For the TxMLS, only deformation in the top 90mm AC layers was considered *and not total rutting*.

The methodology for the theoretical rut ratio (TRR) analysis involved consideration of the temperature and tire pressure to determine the stress for the specific loading configurations of both the MMLS3 and TxMLS. Rutting was assumed proportional to the RP, and based on this hypothesis RPRs were calculated. The second step was to account for temperature differences among the various tests by using G* to determine a temperature correction factor (TCF). It was assumed that rutting is inversely proportional to the G* values at the respective temperatures. This assumption was taken into account by determining a TCF based on the ratios of the respective G* values in Figure 26.
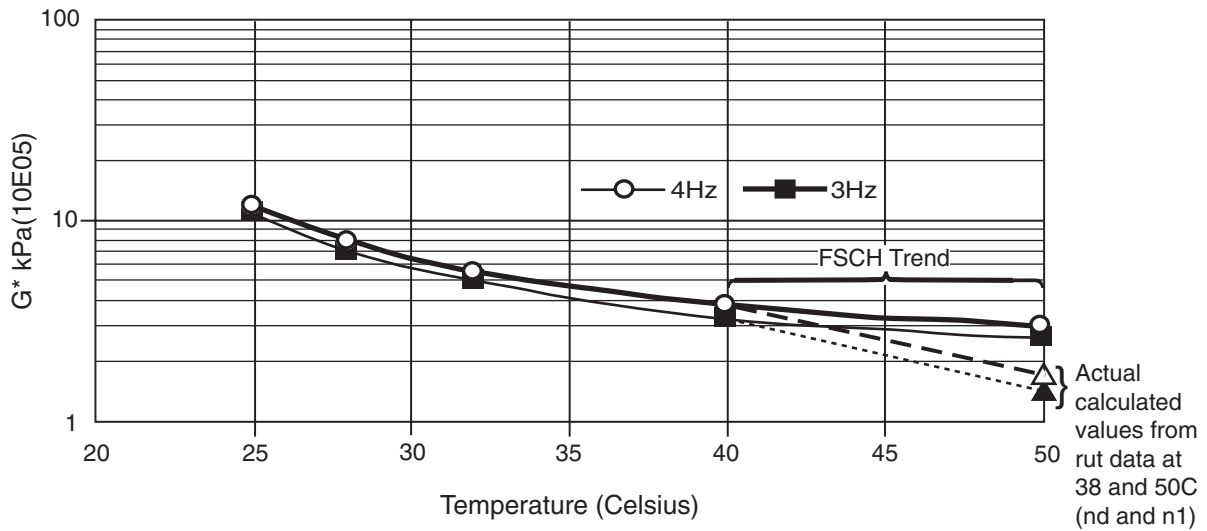
(a) Northbound lane
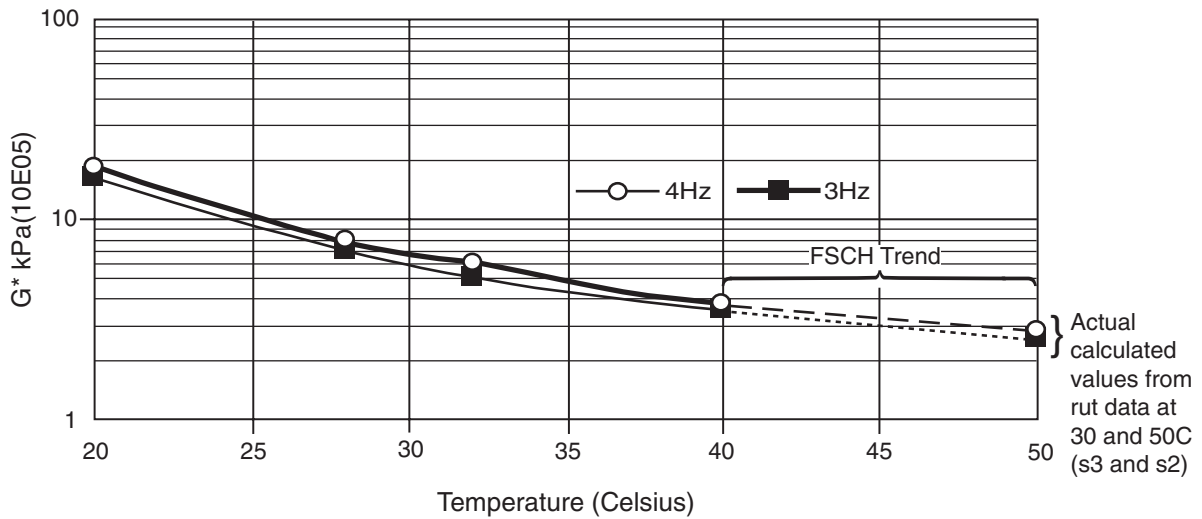
(b) Southbound lane

Figure 26: Shear stiffness (G*) versus temperature

Since the G* values had been determined only up to 40 $^{\circ}$C, values at 50 $^{\circ}$C had to be determined by extrapolation. However, because of the sensitive nature of extrapolation, these values were checked against the results of the MMLS3 tests. It was hypothesized that a pseudo G* could be calculated from the rutting data of two independent MMLS3 tests.

Determination of Pseudo G* Values for the Northbound Test Section

For this analysis, the results for nd (Smit et al. 1999) and n1were used (see Table 4 and Figures 16–20).

1. Rutting Potential Ratio (690kPa/420kPa): nd/n1 = 32.215/20.6 = 1.56

2. Rut of n1 at higher tire pressure, i.e., 690 kPa, 320 k: 1.56*2.165 = 3.38 mm

3. Therefore the actual rut ratio @ 320 k is n1/nd: 3.38/1.3 = 2.6

4. Using G* @ 38 °C (Figure 25[a]) as a basis, we find a "pseudo" G* at 50 °C for MMLS3 (4 Hz) by using the actual rut ratio

i.e., @ 38 °C, G* = 4.06 x 10^5 kPa
@ 50 °C, G* = 4.06 x 10^5 kPa/2.6 = 1.56 x 10^5 kPa

This yields 3 Hz (TxMLS) pseudo G* of about 1.4 x 10^5 kPa @ 50 °C

5.   Temperature Correction Factor (TCF)

G* @ 30.5 °C (Figure 25 [a])/G* @ 50 °C = 5.5 x 10^5 kPa/1.56 x 10^5 kPa = 3.53

Determination of Pseudo G* Values for the Southbound Test Section

For this analysis, the results for s2 and s3 were used (see Table 4 and Figures 16–20).

1. Rutting Potential Ratio (690 kPa/420 kPa): s2/s3 = 1.64

2. Rut of s2 at higher tire pressure, i.e., 690 kPa, 160k: 1.64*1.5 = 2.46 mm

3. Therefore the actual rut ratio @ 160k is s2/s3: 2.46/1.0 = 2.46

4. Using G* @ 30 °C (Figure 25[b]) as a basis, we find a "pseudo" G* at 50 °C for MMLS3 (4 Hz) by using the actual rut ratio

i.e., @ 30 °C, G* = 6.8 x 10^5 kPa
@ 50 °C, G* = 6.8 x 10^5 kPa/2.46 = 2.76 x 10^5 kPa

This yields 3 Hz (TxMLS) pseudo G* about of <u>2.5 x 10^5 kPa</u> @ 50 °C

5. Temperature Correction Factor (TCF)

G* @ 25.5 °C (Figure 25[b])/G* @ 50 °C = 9.0 x 10^5 kPa/2.76x 10^5 kPa = <u>3.26</u>

From the results of the tests on the northbound section, the calculated pseudo G* did not match the extrapolated trend, whereas the results from the southbound section tests fitted closely.

Researchers obtained the TRR by multiplying the RPR with the TCF. For the field rut ratios (FRR), the actual measured rut values at equivalent axles were used. Where insufficient axles had been applied, the extrapolated values were used. The analysis for the comparison is shown in Table 12. Only the upper 90 mm section of the pavement structures was considered.

For the northbound section, the MMLS3:TxMLS RPR was 0.59; for the southbound it was 0.67. The respective TCFs were 3.53 and 3.26. The rut ratios (theoretical versus field) for the northbound sections were approximately 2.1 compared to 1.7 for the MMLS3:TxMLS. In the southbound structure, the values were 2.2 and 2.3, respectively. The latter value was larger than its northern counterpart, possibly because L2 in pad s2 was thinner than L2 in pad n2. The TRR versus FRR ratios were 1.2 and 1.0 for the northbound and southbound sections respectively.

The above methodology was also used to evaluate the actual rut ratios reported by Smit et al. (1999) for their tests with the MMLS3. The results are shown in Table 14. It will be seen that the relationship between the actual rut ratios and those theoretically calculated is 1.3, which is almost the same as that found for the comparison between the MMLS3 and the TxMLS on the northbound lane. The respective theoretical and field rut ratios are shown in column 8 of Tables 12 and 14. These ratios are remarkable, given the different temperature conditions and trafficking. Nonetheless, it is apparent that G* alone does not include all the factors that affect the rut ratios.

Table 14: Comparison of MMLS3 rut ratios in the northbound lane (nd versus nw)

Pad	Calculations		RPR	TCF	TRR	FRR	TRR versus FRR
	Rutting after 1.0 million axles (mm)	RP (MPa*mm)					
nd	1.8	32.22	1.1	2.39	2.6	2.0	1.3
nw	0.9	30.5					

Considering the pilot nature of the project and the low axle counts, these results are very promising. It appears reasonable to use G* ratios as TCFs when estimating the field rut ratio resulting from trafficking. These results support the findings by Anderson et al. (2000).

Material Testing and Characterization

There was a general increase in BSG (densification) on the order of about 2.5% owing to MMLS3 compaction in the hot sections. On the wet pads, a decrease in relative density (~3%) was evident owing to AC degradation and stripping as a result of the effects of water.

Moisture sensitivity test results indicated that both the upper layers (limestone AC and the Dustrol LWAC) of the northbound pavement structure were susceptible to water damage. In the southbound pavement structure, only the second in-situ LWAC layer was expected to be moisture-susceptible. In the field, different results surfaced. The limestone AC proved to be water-resistant, while the Dustrol was very temperature- and water-damage-susceptible. The Remixer was less prone to water damage than the Dustrol and less temperature susceptible than the LWAC. The in-situ LWAC in both the northbound and southbound structures exhibited a similar degree and extent of water damage at equivalent MMLS3 axle loads. The LWAC also appeared to have been the most affected by water in terms of damage.

The average measured ITS strengths of the Remixer and Dustrol were 1,112 kPa and 804 kPa, respectively. The Remixer was thus about 38% stronger than the Dustrol material.

A gain in fatigue life (about 17%) owing to heating and MMLS3 traffic consolidation was evident in the dry, hot pads. However, there was an average loss of about 35% in fatigue life on the wet pads as a result of water damage.

In concurrence with the fatigue results, there was an average decrease of 12% in SCB strength on the wet pads (n3 and s3).

In Situ AC Moduli Measurements

Both PSPA and SASW results indicated a loss in stiffness on the wet pads owing to water damage and a gain in stiffness on the hot pads owing to MMLS3 compaction. There were average losses of about 35% and 9.5% in stiffness on the Dustrol and Remixer, respectively, under wet MMLS3 trafficking.

One factor not considered in the analysis is the fact that the Remixer (1995) is 1 year older than the Dustrol (1996).

CONCLUSIONS

The following conclusions can be drawn from the study on the basis of the above discussions:

Performance in Terms of Rutting and Permanent Deformation

- The Remixer rehabilitation process was more rut-resistant than the Dustrol process. The surface layers of the northbound pavement structure were also less resistant to permanent deformation than those of the southbound structure. These discoveries validate the TxMLS findings.
- Deeper surface rutting was manifested in the northbound structure than in the southbound structure under heated testing, indicating that the northbound structure was more sensitive to temperature than was the southbound structure.
- The theoretical versus field rut ratios (MMLS Mk3:TxMLS) ranged from 1.0 to 1.3. Given the limited nature of the study, and considering all the influencing factors, this finding is considered significant and very promising for future applications of the two machines.
- It was found that the use of G* as a temperature correction factor was a reasonable methodology for use in relating rutting at different temperatures. It was used in this manner to compare the rut ratios between the MMLS3 and TxMLS. However, it appears that the use of the G* does not take into account all the factors that affect the rut ratios.
- In comparing the rutting performance of the top AC layers under the MMLS3 and in the Hamburg test, the researchers found that:
- both indicated the northbound structure to be more rut-susceptible under trafficking.
- the composite upper layers yielded different results. The Hamburg test showed similar behavior for both the northbound and southbound layers, whereas the MMLS3 found the northbound layer to be more rut-susceptible than the southbound layer.
- the MMLS3 showed layer 2 to be more susceptible to temperature in both the northbound and southbound sections. The results of the Hamburg test did not detect this susceptibility.

Performance in Terms of Laboratory Indirect Tension Fatigue Testing

- The Remixer had a poorer fatigue performance than the Dustrol under hot, dry trafficking conditions.
- MMLS3 trafficking with heating had a compaction effect (densification) on the pavement structure, as was evident from the increased BSG of the trafficked cores compared with the untrafficked ones. This densification effect generally increased the fatigue life of the asphalt layers.
- The limestone AC and the lower Remixer layers were less susceptible to water damage than were layers with Dustrol.

  - In both the northbound and southbound structures, the underlying in-situ LWAC exhibited a similar degree of water damage at equivalent MMLS3 axle loads; they were, in fact, the layers most affected by water (in terms of damage), followed by the Dustrol layers.

- Under wet MMLS3 trafficking and equivalent axle loads, the northbound and southbound structures would have similar fatigue life expectancies if water has the same accessibility into the respective LWAC layers during trafficking.
- It is apparent that the fatigue life expectancy of AC materials susceptible to moisture damage is significantly reduced by wet trafficking, so that even light axle loads with high tire pressures (690 kPa) cause substantial damage.
- The indirect tensile fatigue test results of specimens from the wet trafficked pads served as indicators of moisture sensitivity. These results were compared to those established in terms of AASHTO T283. The comparison seems to show that a pavement's ability to pass the prescribed AASHTO T283 specification does not necessarily mean that the AC material will not be damaged by water or will not strip. Likewise, failure to meet the criteria of the specification (TSR≥0.8, as recommended in the new TxDOT and Strategic Highway Research Program [SHRP] procedures) may not necessarily mean that the AC material will fail as a result of water damage under trafficking.
- Of course, these findings relate to the materials tested, and it remains to be determined to what extent they are valid in general.

The fact is that similar forms of distress had already occurred in the outer southbound lane after 3 years of conventional trafficking (i.e., the number of axles applied were far fewer than the number of axles applied during TxMLS testing under ambient conditions).

General

- The profilometer and LDPs were appropriate tools for monitoring the surface rut development and the relative pavement layer deformation, respectively.
- The indirect tensile fatigue testing used in this study proved to be valuable as a tool for monitoring progressive distress of AC owing to traffic and to such environmental factors as heat and water.
- The PSPA and SASW devices were found to be ideal tools for measuring changes in the elastic modulus of the in situ pavement materials. However, it is imperative that one always take into account the temperature at the time of seismic measurement, as the AC modulus is strongly dependent on this factor.

Overall, the research demonstrated that the MMLS3, used in conjunction with nondestructive field and laboratory testing, is a powerful, cost-effective APT device that can effectively evaluate the response and performance of dry, heated, and wet surface layers of full-scale, in-service pavements. The device can also be used to evaluate the performance of different pavement materials. Furthermore, the MMLS3 proved to be a valuable tool for supplementing such full-scale APT devices as the TxMLS.

RECOMMENDATIONS

1. When measuring the in-situ pavement AC moduli using the PSPA or the SASW device, researchers should consider the following guidelines:

   - The AC modulus is strongly dependent on temperature, and a record of the pavement temperature at the time of the measurement is essential. Good seismic readings are obtained within a temperature range of 15 $^{\circ}$C to 30 $^{\circ}$C.
   - Cracked pavement areas should be avoided, given that they can have a negative effect on the PSPA and SASW readings.
   - Better test results are obtained if the pavement surface is flat and smooth.

2. Structural details and material characteristics should always be considered in the selection of test pads so that test pad performance can be properly evaluated. This consideration is particularly important in comparative studies.

3. The results of the Hamburg test were in some instances contrary to the actual performance under MMLS3 trafficking. Based on the fact that MMLS3 trafficking closely simulates real traffic with pneumatic tires, it was concluded that the Hamburg test may have limitations and therefore further comparative studies are needed.

REFERENCES

Anderson, R. M., Huber, G. A., Walker, D. E., and Zhang, X. (2000). "Mixture Testing, Analysis, and Field Performance of Pilot Superpave Projects: The 1992 SPS-9 Mixtures." Preprint. Association of Asphalt Paving Technologists, Reno, Nevada.

Aouad, M. F., Stokoe, K. H., and Briggs, R. C. (1993). "Stiffness of Asphalt Concrete Surface Layer from Stress Wave Measurements." *Transportation Research Record 1384,* Washington, D.C., pp. 29–35.

Epps, J. A. (1969). "Influence of Mixture Variables on the Flexural Fatigue and Tensile Properties of Asphalt Concrete." Doctoral dissertation, University of California, Berkeley.

Huang, Yang, H. (1993). *Pavement Analysis and Design.* Englewood Cliffs, New Jersey.

Hugo, Fred, Smit, A. D. F., and Epps, Amy (1999[a]). "Model APT in the Field, Paper: CS6-6." Paper presented at the International Conference on Accelerated Pavement Testing in Reno, Nevada, October 18–20.

Hugo, Fred, Fults, Ken, Chen, Dar-Hao, Smit, A. D. F., and Bilyeu, John (1999[b]). "An Overview of the TxMLS Program and Lessons, Paper GS3-4." Paper presented at the International Conference on Accelerated Pavement Testing in Reno, Nevada, October 18–20.

Hugo, Fred, Chen, Dar-Hao, Smit, A. D. F., and Bilyeu, John (1999[c]). "Report on a Comparison of the Effectiveness of Two Pavement Strategies on US 281 near Jacksboro (1814-1)." Draft report prepared for the Texas Department of Transportation by the Center for Transportation Research, The University of Texas at Austin.

Lee, N. K. J., Hugo, F., and Stokoe, K. H. (1997). "Detection and Monitoring of Cracks in Asphalt Pavement under Texas Mobile Load Simulator Testing." *Transportation Research Record 1570,* Washington, D.C.

Li, Y., and Nazarian, S. (1994). "Evaluation of Aging of Hot-Mix Asphalt Using Wave Propagation Techniques." STP 1265, ASTM, Philadelphia, PA, pp. 166–179.

Muller, Johan F. P. (1999). *MMLS3 Traffic Simulator. Operators Manual.* Stellenbosch.

Raithby, K. D., and Ramshaw, J. T. (1972). "Effect of Secondary Compaction on the Fatigue Performance of Rolled Asphalt." TRRL-LR 496, Crowthorne, England.

Shell Bitumen (1998). *BISAR 3.0.* Shell International Oil Products BV. London.

Smit, A. D. F., Hugo, Fred, and Epps, Amy (1999). "Report on the First Jacksboro MMLS3 Tests (1814-2)." Research Project 0-1814. Draft Report prepared for the Texas Department of Transportation by the Center for Transportation Research, The University of Texas at Austin.

Tangella, Rao S. C. S., Graus, J., Deacon, J. A., and Monismith, C. L. (1990). "Summary Report on Fatigue Response of Asphalt Mixtures." Berkeley, California.